

1 **The hidden role of dissolved organic carbon in the**  
2 **biogeochemical cycle of carbon in modern redox-stratified**  
3 **lakes**

4 Robin Havas<sup>a,\*</sup>, Christophe Thomazo<sup>a,b</sup>, Miguel Iniesto<sup>c</sup>, Didier Jézéquel<sup>d</sup>, David Moreira<sup>e</sup>, Rosaluz Tavera<sup>e</sup>,  
5 Jeanne Caumartin<sup>f</sup>, Elodie Muller<sup>f</sup>, Purificación López-García<sup>e</sup>, Karim Benzerara<sup>f</sup>  
6

7 <sup>a</sup> Biogéosciences, CNRS, Université de Bourgogne Franche-Comté, 21 000 Dijon, France

8 <sup>b</sup> Institut Universitaire de France, 75005 Paris, France

9 <sup>c</sup> Ecologie Systématique Evolution, CNRS, Université Paris-Saclay, AgroParisTech, 91190 Gif-sur-Yvette,  
10 France

11 <sup>d</sup> IPGP, CNRS, Université Paris Cité, 75005 Paris, and UMR CARTELE, INRAE & USMB, France

12 <sup>e</sup> Departamento de Ecología y Recursos Naturales, Universidad Nacional Autónoma de México, México

13 <sup>f</sup> Sorbonne Université, Muséum National d'Histoire Naturelle, CNRS, Institut de Minéralogie, de Physique des  
14 Matériaux et de Cosmochimie (IMPMC), 75005 Paris, France.  
15

16

17

18 \* *Correspondence to:* Robin Havas ([robin.havas@gmail.com](mailto:robin.havas@gmail.com))

19

20

21

22

23

*Keywords: Carbon cycle; isotopic fractionation; DOC; Precambrian analogues*

24 **Abstract.** The dissolved organic carbon (DOC) reservoir plays a critical role in the C cycle of marine and  
25 freshwater environments because of its size and implication in many biogeochemical reactions. Although it is  
26 poorly constrained, its importance in ancient Earth's C cycles is also commonly invoked. Yet DOC is rarely  
27 quantified and characterized in modern stratified analogues. In this study, we investigated the DOC reservoirs of  
28 four redox-stratified alkaline crater lakes in Mexico. We analyzed the concentrations and isotopic compositions of  
29 DOC throughout the four water columns and compared them with existing data on dissolved inorganic and  
30 particulate organic C reservoirs (DIC and POC). The four lakes have high DOC concentrations with great  
31 variability between and within the lakes (averaging  $2 \pm 4$  mM; 1SD, n=28; i.e. from ~ 15 to 160 times the amount  
32 of POC). The  $\delta^{13}\text{C}_{\text{DOC}}$  signatures also span a broad range of values from -29.3 to -8.7 ‰ (with as much as 12.5 ‰  
33 variation within a single lake). The prominent DOC peaks (up to 21 mM), together with their associated isotopic  
34 variability, are interpreted as reflecting oxygenic and/or anoxygenic primary productivity through the release of  
35 excess fixed carbon in three of the lakes (La Alberca de los Espinos, La Preciosa, and Atexcac). By contrast, the  
36 variability of [DOC] and  $\delta^{13}\text{C}_{\text{DOC}}$  in the case of Lake Alchichica is mainly explained by the partial degradation of  
37 organic matter and accumulation of DOC in anoxic waters. The DOC records detailed metabolic functions such as  
38 active DIC-uptake and DIC-concentrating mechanisms, which cannot be inferred from DIC and POC analyses  
39 alone, but which are critical to the understanding of carbon fluxes from the environment to the biomass.  
40 Extrapolating our results to the geological record, we suggest that anaerobic oxidation of DOC may have caused  
41 the very negative C isotope excursions in the Neoproterozoic. It is however unlikely that a large oceanic DOC  
42 reservoir could outweigh the entire oceanic DIC reservoir. This study demonstrates how the analysis of DOC in  
43 modern systems deepens our understanding of the C cycle in stratified environments and helps to set boundary  
44 conditions for the Earth's past oceans.

45

46

## 47 1. INTRODUCTION

48 Dissolved organic carbon (DOC) is a major constituent of today's marine and freshwater environments (e.g.  
49 Ridgwell and Arndt, 2015; Brailsford, 2019). It is an operationally defined fraction of aqueous organic carbon  
50 within a continuum of organic molecules spanning a broad range of sizes, compositions, degrees of reactivity, and  
51 bioavailability (Kaplan et al., 2008; Hansell, 2013; Beaupré, 2015; Carlson and Hansell, 2015; Brailsford, 2019).  
52 Oceanic DOC is equivalent to the total amount of atmospheric carbon (Jiao et al., 2010; Thornton, 2014) and  
53 represents the majority of freshwater organic matter (Kaplan et al., 2008; Brailsford, 2019). The DOC reservoir is  
54 (i) at the base of many trophic chains (Bade et al., 2007; Hessen and Anderson, 2008; Jiao et al., 2010; Thornton,  
55 2014), (ii) key in physiological and ecological equilibria (Hessen and Anderson, 2008) and (iii), has a critical role  
56 for climate change as a long-term C storage reservoir (Jiao et al., 2010; Hansell, 2013; Thornton, 2014; Ridgwell  
57 and Arndt, 2015). Although isotopic signatures are a powerful and widespread tool in biogeochemical studies, the  
58 use of DOC isotopes has been relatively limited owing to technical difficulties (Cawley et al., 2012; Barber et al.,  
59 2017). Radioisotopes or labeled stable isotopes of DOC have been used to date and retrace DOC compounds in  
60 diverse aquatic environments (e.g. Repeta and Aluwihare, 2006; Bade et al., 2007; Kaplan et al., 2008; Brailsford,  
61 2019). Studies featuring natural abundances of DOC stable isotope data (i.e.  $\delta^{13}\text{C}_{\text{DOC}}$ ) mainly used them to  
62 discriminate between different source endmembers (e.g. terrestrial vs. autochthonous) (e.g. Cawley et al., 2012;  
63 Santinelli et al., 2015; Barber et al., 2017). After a pioneer study by Williams and Gordon (1970), few studies have  
64 used natural DOC stable isotope compositions to explore processes intrinsically related to its production and  
65 recycling. Recently, Wagner et al. (2020) reaffirmed the utility of stable isotopes to investigate DOC biosynthesis,  
66 degradation pathways, and transfer within the foodweb.

67 Several studies have suggested a significant role for the DOC reservoir throughout geological time, when it would  
68 have been much larger in size and impacting various phenomena, including: the regulation of climate and  
69 glaciations during the Neoproterozoic (e.g. Peltier et al., 2007), the paleoecology of Ediacaran Biota and its early  
70 complex life forms (e.g. Sperling et al., 2011), the oxygenation of the ocean through innovations of eukaryotic life  
71 near the Neoproterozoic-Cambrian transition (e.g. Lenton and Daines, 2018), and the perturbation of the C cycle  
72 recorded in  $\delta^{13}\text{C}$  sedimentary archives from the Neoproterozoic to the Phanerozoic (e.g. Rothman et al., 2003; Fike  
73 et al., 2006; Sexton et al., 2011; Ridgwell and Arndt, 2015).

74 The contribution of DOC reservoirs to the past and modern Earth's global climate and biogeochemical cycles  
75 remains poorly constrained (Jiao et al., 2010; Sperling et al., 2011; Dittmar, 2015; Fakhraee et al., 2021) and the  
76 existence and consequences of a large ancient oceanic DOC are still debated (e.g. Jiang et al., 2010, 2012; Ridgwell  
77 and Arndt, 2015; Li et al., 2017; Fakhraee et al., 2021). Thus, in addition to modeling approaches (e.g. Shi et al.,  
78 2017; Fakhraee et al., 2021), the understanding of DOC-related processes in the past anoxic and redox-stratified  
79 oceans (Lyons et al., 2014; Havig et al., 2015; Satkoski et al., 2015) should rely on the characterization of DOC  
80 dynamics in comparable modern analogues (Sperling et al., 2011). Although many studies have explored the C  
81 cycle of modern redox-stratified environments (e.g. Crowe et al., 2011; Kuntz et al., 2015; Posth et al., 2017;  
82 Schiff et al., 2017; Havig et al., 2018; Cadeau et al., 2020; Saini et al., 2021; Petrash et al., 2022), very few have  
83 analyzed DOC and even fewer have measured its stable isotope signature (Havig et al., 2018).

84 In this study, we characterize the DOC reservoir of four modern redox-stratified alkaline crater lakes from the  
85 Trans-Mexican Volcanic Belt (Ferrari et al., 2012) and its role within the C cycle of these environments. We report

86 DOC concentration and isotopic composition at multiple depths in the four water columns, and discuss these results  
87 in the context of physico-chemical parameters (temperature, dissolved oxygen, chlorophyll a, and nutrient  
88 concentrations), and the isotopic composition of dissolved inorganic and particulate organic carbon (DIC, POC),  
89 all measured in the same lakes and from the same water samples as in Havas et al. (submitted). The four lakes  
90 show distinct water chemistries, along an alkalinity/salinity gradient (Zeyen et al., 2021), with diverse planktonic  
91 microbial communities (Iniesto et al., 2022; Havas et al., submitted). These characteristics allow us to examine the  
92 effect of specific environmental and ecological constraints on the production and recycling of DOC in redox  
93 stratified environments. We then present how the analysis of DOC deepens our understanding of the C cycle in  
94 these lakes, compared to more classical DIC and POC analyses. Finally, the production and fate of the DOC  
95 reservoir in these modern analogues is used to discuss the potential role of DOC in past perturbations of the  
96 sedimentary C isotope record from the Neoproterozoic and Phanerozoic.

97

## 98 2. SITE DESCRIPTION

99 The main characteristics of the geological, climatic and limnological context of the lakes under study are presented  
100 here, but a more detailed description is available in Havas et al. (submitted).

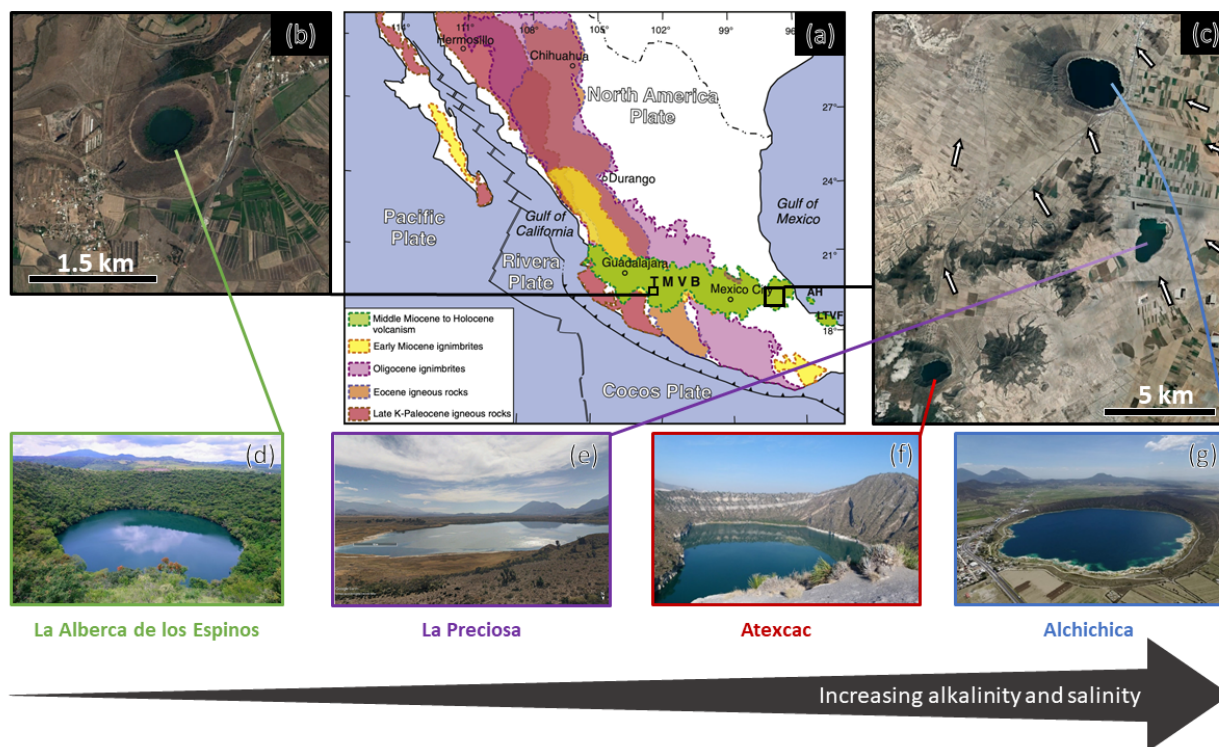
101 The four lakes are volcanic maars formed after phreatic, magmatic and phreatomagmatic explosions, and are  
102 located in the Trans-Mexican Volcanic Belt (TMVB, Fig. 1). The first lake, La Alberca de los Espinos, is located  
103 at the margin of the Zacapu tectonic lacustrine basin in the Michoacán-Guanajuato Volcanic Field (MGVF), in the  
104 western-central part of the TMVB (Fig. 1). The other three (La Preciosa, Atexcac, and Alchichica) are located  
105 within the same zone (~ 50 km<sup>2</sup>) of the Serdan-Oriental Basin (SOB), in the easternmost part of the TMVB (Fig. 1).  
106 La Alberca, with a temperate semi-humid climate, is predominantly underlain by andesitic rocks (Siebe et al.,  
107 2012, 2014). By contrast, Alchichica shows much higher evaporation than precipitation rates, reflecting the  
108 temperate sub-humid to temperate arid climate experienced by the SOB lakes (Silva-Aguilera et al., 2022). These  
109 lakes overlie calcareous and basaltic/andesitic basement rocks (Carrasco-Núñez et al., 2007; Chako Tchamabé et  
110 al., 2020).

111 These variations in geological context and hydrological processes generate a gradient of water chemical  
112 compositions, where salinity, alkalinity and DIC increase in the following order: (i) Lake La Alberca, (ii) La  
113 Preciosa, (iii) Atexcac, and (iv) Alchichica (Zeyen et al., 2021). The four lakes are alkaline with pH values around  
114 9. Under these conditions, DIC is composed of HCO<sub>3</sub><sup>-</sup>/CO<sub>3</sub><sup>2-</sup> ions with minor amounts of CO<sub>2(aq)</sub> (< 0.5 %). This  
115 favors the precipitation of microbialite deposits, which are found in the four systems but more abundantly as  
116 alkalinity increases (Zeyen et al., 2021).

117 The four lakes are defined as warm monomictic with anoxic conditions prevailing in the bottom waters during  
118 most of the year (i.e. one mixing period per year, during winter; Armienta et al., 2008; Macek et al., 2020; Havas  
119 et al., submitted). They are all “closed lakes” with no inflow or outflow of surficial waters and are thus fed by rain  
120 and groundwater only.

121 Atexcac is the most oligotrophic of the three SOB lakes (Lugo et al., 1993; Vilaclara et al., 1993; Sigala et al.,  
122 2017). Chlorophyll a data from May 2019 (Fig. 2), based on mean and maximum value categories (OECD, 1982),  
123 indicate ultra-oligotrophic conditions for Atexcac (≤ 1 and 2 µg/L, respectively), oligotrophic for Alchichica (≤ 2

124 and 6  $\mu\text{g/L}$ , respectively), intermediate between oligo- and mesotrophic for La Alberca ( $\leq 3$  and 4.5  $\mu\text{g/L}$ ,  
 125 respectively) and “low” mesotrophic for La Preciosa ( $\leq 3$  and 9  $\mu\text{g/L}$ , respectively). Total dissolved P  
 126 concentrations from May 2019 show similar values for the three SOB lakes close to the surface (increasing in the  
 127 anoxic zone of Alchichica) but much higher values for La Alberca (Havas et al., submitted). This pattern was  
 128 observed during previous sampling campaigns (Zeyen et al., 2021). La Alberca is surrounded by more vegetation,  
 129 which could favor the input of nutrients to this lake. La Preciosa and La Alberca are thus the least oligotrophic of  
 130 the four lakes. Importantly, although differences in trophic status exist between the four lakes, they are more  
 131 oligotrophic than eutrophic.



132  
 133 Figure 1. Geographical location and photographs of the four crater lakes. (a) Geological map from Ferrari et al.  
 134 (2012) with black squares showing the location of the four studied lakes within the Trans-Mexican Volcanic Belt  
 135 (TMVB). (b, c) Close up © Google Earth views of La Alberca de los Espinos and the Serdan-Oriental Basin  
 136 (SOB). The white arrows represent the approximate groundwater flow path (based on Silva-Aguilera, 2019). (d-  
 137 g) Photographs of the four lakes (d from © Google Image [‘enamoredemexicowebiste’], e from © Google Earth  
 138 street view, and g from © ‘Agencia Es Imagen’). Figure from Havas et al. (submitted).

139

### 140 3. METHOD

#### 141 3.1. Sample Collection

142 All samples were collected in May 2019. Samples for DOC analyses were collected at different depths from the  
 143 surface to the bottom of the water columns, particularly where the physico-chemical parameters showed  
 144 pronounced variation (e.g. at the chemocline and turbidity peaks; Fig. 2 and Table 1). Water samples were collected  
 145 with a Niskin bottle. For comparison with DIC and POC data, the DOC was analyzed on the same Niskin sampling  
 146 as in Havas et al. (submitted), except where indicated (Fig. 4; Tables 1 and 2). Analyses of DOC and major, minor,

147 and trace ions were carried out after water filtration at 0.22  $\mu\text{m}$ , directly in the field with Filtropur S filters pre-  
148 rinsed with lake water. Details about the sampling procedure and analysis of the physico-chemical parameters, as  
149 well as DIC and POC measurements, are reported in Havas et al. (submitted).

150

### 151 **3.2. Dissolved organic carbon (DOC) concentration and isotope measurements**

152 Filtered solutions were acidified to a pH of  $\sim 1-2$  to degas all the DIC and leave DOC as the only C species in  
153 solution. The bulk DOC was analyzed directly from the acidified waters (i.e. all organic C molecules smaller than  
154 0.22  $\mu\text{m}$ ). Bulk concentration was measured with a Vario TOC at the Laboratoire Biogéosciences (Dijon),  
155 calibrated with a range of potassium hydrogen phthalate (Acros®) solutions. Before isotopic analysis, DOC  
156 concentration of the samples was adjusted to match international standards at 5 ppm (USGS 40 glutamic acid and  
157 USGS 62 caffeine). Isotopic compositions were measured at the Laboratoire Biogéosciences using an IsoTOC  
158 (Elementar, Hanau, Germany), running under He-continuous flow and coupled with an IsoPrime stable isotope  
159 ratio mass spectrometer (IRMS; Isoprime, Manchester, UK). Samples were stirred with a magnetic bar and flushed  
160 with He before injection of 1 mL sample aliquots (repeated 3 times). The DOC was then converted into gaseous  
161  $\text{CO}_2$  by combustion at 850  $^\circ\text{C}$ , quantitatively oxidized by copper oxide and separated from other combustion  
162 products in a reduction column and a water condenser. This  $\text{CO}_2$  was transferred to the IRMS via an open split  
163 device. To avoid a significant memory effect between consecutive analyses, each sample (injected and measured  
164 three times) was separated by six injections of deionized water and the first sample measurement was discarded.  
165 Average  $\delta^{13}\text{C}_{\text{DOC}}$  reproducibility was 1.0 ‰ for standards and 0.5 ‰ for samples (1SD). The average  
166 reproducibility for sample [DOC] measurements was 0.3 mM, and blank tests were below the detection limit.

167 In addition to DOC measurements, we calculated the “Total carbon concentration” as the sum of DOC, DIC, and  
168 POC concentrations, with DIC and POC data from Havas et al. (submitted). The corresponding isotopic  
169 composition ( $\delta^{13}\text{C}_{\text{Total}}$ ) was calculated as the weighted average of the three  $\delta^{13}\text{C}$ . The DIC and POC isotope data  
170 were also used to calculate isotopic differences with  $\delta^{13}\text{C}_{\text{DOC}}$ , expressed in the  $\Delta^{13}\text{C}$  notation. The values for  $\delta^{13}\text{C}_{\text{DIC}}$   
171 and  $\delta^{13}\text{C}_{\text{POC}}$  are detailed in Havas et al. (submitted) and summarized in the results section.

172

## 173 **4. RESULTS**

174 The water columns of the four lakes were clearly stratified in May 2019 (Fig. 2; Havas et al., submitted). The epi-  
175 , meta-, and hypo-limnion layers of each lake were identified based on the thermocline depths, and correspond to  
176 the oxygen-rich, intermediate, and oxygen-poor layers in the four lakes, although the oxycline in La Preciosa is  
177 slightly thinner than the thermocline ( $\sim 5$  vs. 8 m). In the following, DIC, POC,  $\text{O}_2$ , chlorophyll a (Chl a),  $\text{NH}_4$ , P  
178 and  $\text{CO}_{2(\text{aq})}$  data are also presented.

179

### 180 **4.1. Lake La Alberca de los Espinos**

181 Bulk DOC had a concentration of  $\sim 0.4$  mM throughout the water column, except at 7 and 17 m, where it peaked  
182 at 1.0 and 1.7 mM, respectively (Fig. 3). Its isotopic composition ( $\delta^{13}\text{C}_{\text{DOC}}$ ) was comprised between -27.2 and -

183 25.1 ‰ except at 7 m, where it reached -14.7 ‰ (Fig. 3). It represented ~8% of total carbon on average, and 93%  
 184 of the organic carbon present in the water column. Total C concentration increased downward from about 7 to  
 185 9 mM. The  $\delta^{13}\text{C}_{\text{total}}$  decreased from -3.9 to -7.9 ‰ between 5 and 17 m and then increased to -3.2 ‰ at 25 m  
 186 (Table 1). The isotopic difference between DOC and DIC ( $\Delta^{13}\text{C}_{\text{DOC-DIC}}$ ) was between -21.2 and -25.2 ‰, except  
 187 at 7 m depth, where it peaked to -12.4 ‰ (Fig. 4; Table 2). The  $\Delta^{13}\text{C}_{\text{DOC-POC}}$  values were comprised between -1.5  
 188 and +3.1 ‰, except at 7 m depth, where DOC was enriched in  $^{13}\text{C}$  by ~11.5 ‰ (Fig. 4; Table 2). The DIC  
 189 concentration and  $\delta^{13}\text{C}_{\text{DIC}}$  averaged  $7.5 \pm 0.7$  mM and  $-2.9 \pm 0.8$  ‰; POC concentration and  $\delta^{13}\text{C}_{\text{POC}}$  averaged  
 190  $0.04 \pm 0.02$  mM and  $-27.1 \pm 1.3$  ‰. Dissolved oxygen showed a stratified profile with an oxycline layer  
 191 transitioning from O<sub>2</sub>-saturated to O<sub>2</sub>-depleted conditions between 5 and 12 m depths (Fig. 2). Chl a concentration  
 192 showed three distinct peaks at ~7.5, 12.5 and 17.5 m depths, all reaching ~4 µg/L (Fig. 2). The average NH<sub>4</sub><sup>+</sup> and  
 193 P concentrations were 3.9 and 11.3 µM, respectively. The activity of CO<sub>2(aq)</sub> was 10<sup>-5.00</sup> at 7 m depth and increased  
 194 to 10<sup>-3.40</sup> at the bottom of the lake.  
 195

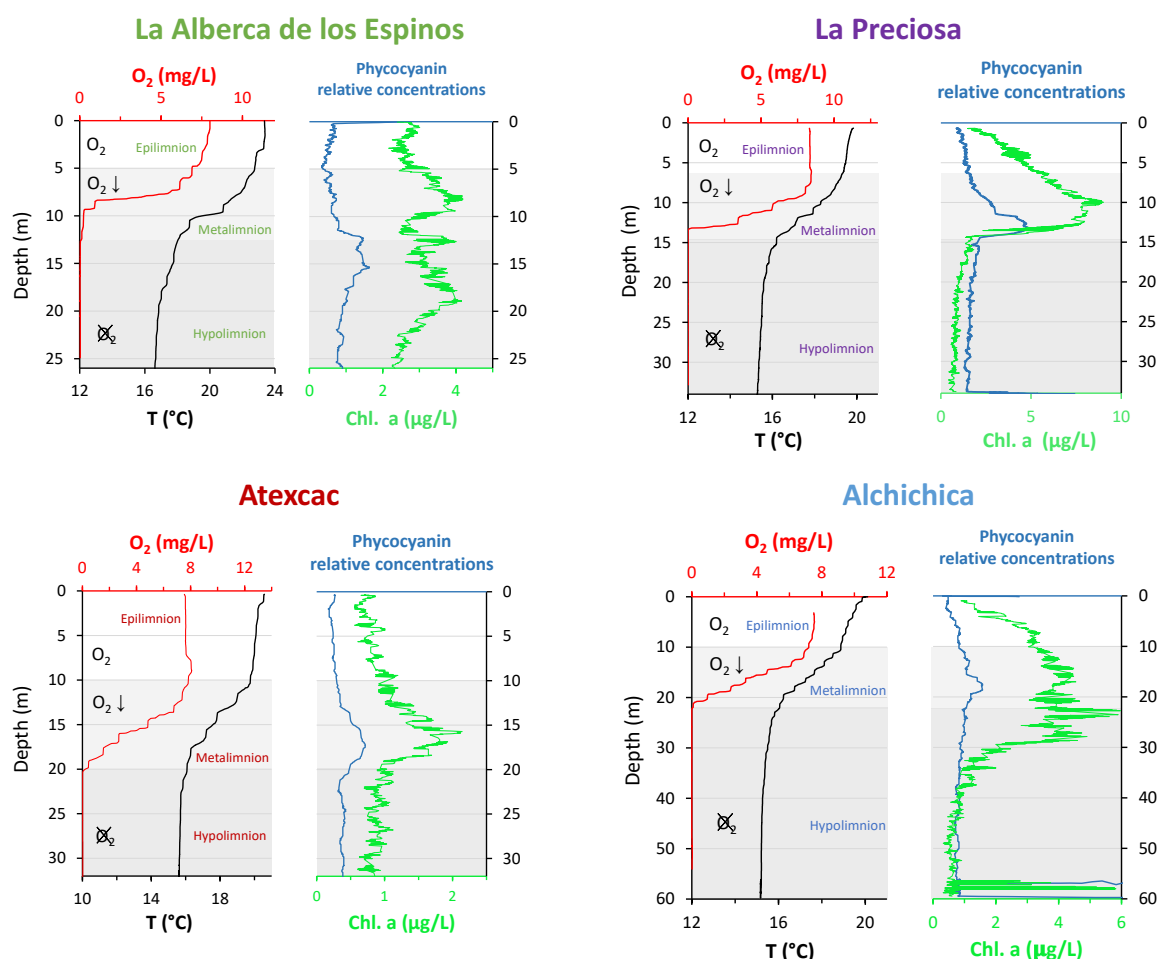


Figure 2. Physico-chemical parameter depth profiles of La Alberca de los Espinos, La Preciosa, Atexcac, and Alchichica: dissolved oxygen concentration (mg/L), water temperature (°C), phycoerythrin and chlorophyll a pigments (µg/L). Absolute values for phycoerythrin concentrations were not determined; only relative variations are represented (with increasing concentrations to the right). Epi-, meta- and hypo-limnion layers are represented for each lake by the white, gray, and dark gray areas, based on temperature profiles with the metalimnion corresponding to the thermocline. The three layers match the oxygen-rich, intermediate, and oxygen-poor zones, except in La Preciosa). Original data from Havas et al. (submitted).

## 196 4.2. Lake La Preciosa

197 Bulk DOC had a concentration of  $\sim 0.5$  mM throughout the water column except at 12.5 m, where it peaked at  
198 1.6 mM. The  $\delta^{13}\text{C}_{\text{DOC}}$  was  $-25.9 \pm 0.4$  ‰ throughout the water column except between 12.5 and 15 m, where it  
199 reached  $-20.0$  ‰ (Fig. 3). The DOC represented  $\sim 3\%$  of the total carbon on average, and 91% of the organic  
200 carbon present in the water column. The total C concentration was relatively stable at  $\sim 13.8$  mM, while  $\delta^{13}\text{C}_{\text{total}}$   
201 was centered around  $-1$  ‰ with a decrease to  $-2.8$  ‰ at 12.5 m (Table 1). The  $\Delta^{13}\text{C}_{\text{DOC-DIC}}$  values were very stable  
202 with depth around  $-26$  ‰, but markedly increased at 12.5 m up to  $-19.8$  ‰. (Fig. 4; Table 2). The  $\Delta^{13}\text{C}_{\text{DOC-POC}}$   
203 values decreased from  $\sim 1.3$  ‰ in the upper waters to  $\sim -0.4$  ‰ in the bottom waters but showed a peak to  $+7.1$  ‰  
204 at a depth of 12.5 m (Fig. 4; Table 2). The DIC concentration and  $\delta^{13}\text{C}_{\text{DIC}}$  averaged  $13.0 \pm 0.8$  mM and  $-0.2 \pm 0.3$  ‰;  
205 POC concentration and  $\delta^{13}\text{C}_{\text{POC}}$  averaged  $0.05 \pm 0.02$  mM and  $-26.1 \pm 1.4$  ‰. Dissolved oxygen showed a stratified  
206 profile with an oxycline layer transitioning from  $\text{O}_2$ -saturated to  $\text{O}_2$ -depleted conditions between 8 and 14 m depths  
207 (Fig. 2). The Chl a concentration showed a large peak at  $\sim 10$  m, reaching  $9$   $\mu\text{g/L}$  (Fig. 2). The average  $\text{NH}_4^+$  and  
208 P concentrations were  $1.9$  and  $0.2$   $\mu\text{M}$ , respectively. The activity of  $\text{CO}_{2(\text{aq})}$  averaged  $10^{-4.57}$ .

209

## 210 4.3. Lake Atexcac

211 Bulk DOC had a concentration of  $\sim 1.1$  mM throughout the water column except at 16 and 23 m, where it reached  
212  $7.7$  and  $20.8$  mM, respectively. The  $\delta^{13}\text{C}_{\text{DOC}}$  increased from  $-20.0$  to  $-8.7$  ‰ between 5 and 23 m, decreasing to  $-$   
213  $11.2$  ‰ at 30 m. It represented about 16% of the total carbon on average, and 98 % of the organic carbon present  
214 in the water column. Total C concentrations and  $\delta^{13}\text{C}_{\text{total}}$  are centered around  $27.7$  mM and  $-0.6$  ‰ with a clear  
215 increase to  $38.9$  mM and decrease to  $-2.7$  ‰ at 23 m, respectively. The  $\Delta^{13}\text{C}_{\text{DOC-DIC}}$  values significantly increased  
216 from the surface ( $-20.4$  ‰) to the hypolimnion ( $\sim -11.4$  ‰). The DOC isotope compositions were strictly and  
217 significantly less negative than POC (i.e. enriched in heavy  $^{13}\text{C}$ ), with  $\Delta^{13}\text{C}_{\text{DOC-POC}}$  reaching as much as  $+17.9$  ‰  
218 at the depth of 23 m (Fig. 4; Table 2). The DIC concentration and  $\delta^{13}\text{C}_{\text{DIC}}$  averaged  $25.7 \pm 0.9$  mM and  $0.5 \pm 0.3$  ‰;  
219 POC concentration and  $\delta^{13}\text{C}_{\text{POC}}$  averaged  $0.04 \pm 0.02$  mM and  $-27.7 \pm 1.1$  ‰. Dissolved oxygen showed a stratified  
220 profile with an oxycline layer transitioning from  $\text{O}_2$ -saturated to  $\text{O}_2$ -depleted conditions between 10 and 20 m  
221 depths (Fig. 2). Chl a concentration showed a small peak at 16 m, reaching  $2$   $\mu\text{g/L}$  (Fig. 2). The average  $\text{NH}_4^+$  and  
222 P concentrations were  $2.5$  and  $0.3$   $\mu\text{M}$ , respectively. The activity of  $\text{CO}_{2(\text{aq})}$  averaged  $10^{-4.27}$ .

223

## 224 4.4. Lake Alchichica

225 Bulk DOC had a concentration of  $\sim 0.5$  mM throughout the water column, except in the hypolimnion, where it  
226 reached up to  $5.4$  mM. The  $\delta^{13}\text{C}_{\text{DOC}}$  varied from  $-29.3$  to  $-25.1$  ‰, with maximum values found in the hypolimnion  
227 (Fig. 3). The DOC represented about 5 % of the total carbon on average, and 93 % of the organic carbon present  
228 in the water column. Total carbon concentration depth profile roughly followed that of DOC, while  $\delta^{13}\text{C}_{\text{total}}$  was  
229 between  $-0.2$  and  $1.6$  ‰ throughout the water column, except in the lower part of the hypolimnion, where it  
230 decreased to  $-2.3$  ‰ (Table 1). The isotopic difference between DOC and DIC ( $\Delta^{13}\text{C}_{\text{DOC-DIC}}$ ) was slightly smaller  
231 in the hypolimnion and was comprised between  $-26.7$  and  $-30.9$  ‰. The DOC isotope compositions were more  
232 negative than POC, with  $\Delta^{13}\text{C}_{\text{DOC-POC}}$  values between  $-0.7$  and  $-3.5$  ‰ (Fig. 4; Table 2). The DIC concentration  
233 and  $\delta^{13}\text{C}_{\text{DIC}}$  averaged  $34.6 \pm 0.6$  mM and  $1.7 \pm 0.2$  ‰; POC concentration and  $\delta^{13}\text{C}_{\text{POC}}$  averaged  $0.01 \pm 0.04$  and  $-$



234 25.6 ± 1.0 ‰. Dissolved oxygen showed a stratified profile with an oxycline layer transitioning from O<sub>2</sub>-saturated  
 235 to O<sub>2</sub>-depleted conditions between ~10 and 20 m depths (Fig. 2). Chl a showed a broad peak between ~ 10 and  
 236 30 m, averaging 4 µg/L and with a narrow maximum of 6 µg/L (Fig. 2). The average NH<sub>4</sub><sup>+</sup> and P concentrations  
 237 were 4.3 and 1.5 µM, respectively. The activity of CO<sub>2(aq)</sub> averaged 10<sup>-4.53</sup>.

238  
 239  
 240

Lake	Sample	DOC	Total Carbon	δ <sup>13</sup> C <sub>DOC</sub>	δ <sup>13</sup> C <sub>Total</sub>
		mmoles/L		‰	
La Alberca de Los Espinosa	Albesp 5m	0.4	7.2	-26.7	-3.9
	Albesp 7m	1.0	8.1	-14.7	-3.9
	Albesp 10m	0.4	7.6	-25.2	-5.1
	Albesp 17m	1.7	9.0	-26.3	-7.9
	Albesp 20m	0.4	8.4	-25.1	-4.5
	Albesp 25m	0.4	9.2	-27.2	-3.2
La Preciosa	LP 5m	0.5	14.0	-25.4	-0.9
	LP 8m	0.9		ND.	ND.
	LP 10m	0.3	13.7	-25.7	-0.4
	LP 12.5m	1.6	13.2	-20.0	-2.8
	LP 15m	0.5	13.9	-24.0	-1.3
	LP 20m	0.3	13.6	-26.2	-1.0
	LP 31m	0.3	13.6	-26.2	-0.9
Atexcac	ATX 5m	0.92	27.4	-20.0	-0.4
	ATX 10m	1.8	28.1	-15.5	-0.7
	ATX 16m	7.8	34.7	ND.	ND.
	ATX 23m	21.0	45.2	-8.7	-3.6
	ATX 30m	0.7	26.4	-11.2	-0.1
Alchichica	AL 5m	0.7	35.8	ND.	ND.
	AL 10m	0.4	33.5	-28.3	1.6
	AL 20m	0.4	35.0	-29.3	1.3
	AL 30m	0.4	35.1	-28.3	1.2
	AL 35m	2.3	37.2	-26.8	-0.2
	AL 40m	2.2	37.0	-25.8	-0.1
	AL 50m	5.0	39.8	-25.1	-1.8
	AL 55m	0.5	35.3	-27.6	1.1
	AL 58m	5.4	40.2	-27.7	-2.3
AL 60m	0.7	35.3	-26.1	1.0	

241  
 242 Table 1  
 243 Concentration and isotopic composition of dissolved organic carbon (DOC). Total carbon concentration is the  
 244 sum of DOC, DIC, and POC reservoirs. For LP 8m, [DIC] was not measured, and the total carbon concentration  
 245 was not calculated. The DIC and POC were determined by Havas et al. (submitted). The δ<sup>13</sup>C<sub>Total</sub> is the weighted  
 246 average of the three δ<sup>13</sup>C. ND: non-determined.

247

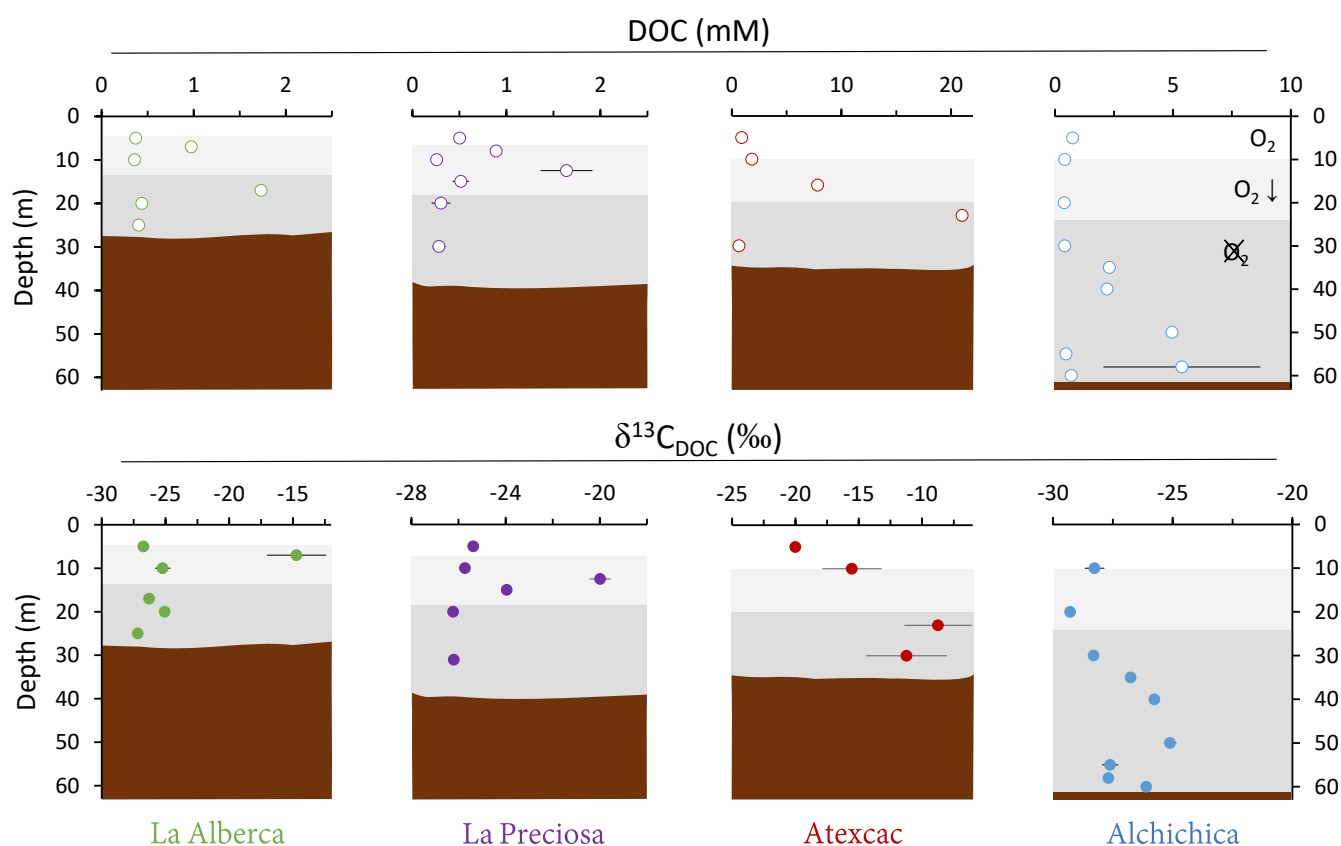


Figure 3. Vertical profiles of concentration and isotopic composition of dissolved organic carbon (DOC) throughout the water columns of the studied lakes: La Alberca de los Espinos, La Preciosa, Atexcac, and Alchichica. Concentration is in  $\text{mmol.L}^{-1}$  (mM) and isotopic composition in ‰ vs. VPDB. The white, gray, and dark gray shading is as in Fig. 2. The brown shading symbolizes the presence of sediment at the bottom of the water columns (showing the greater water depth in Lake Alchichica).

248

## 249 5. DISCUSSION

250

251 The four Mexican lakes studied here have a high DOC content but very different profiles and signatures for [DOC]  
 252 and  $\delta^{13}\text{C}_{\text{DOC}}$  (Fig. 3). Evaporation may increase DOC concentration (Anderson and Stedmon, 2007; Zeyen et al.,  
 253 2021), but would not explain the significant intra-lake DOC variability with depth. It is likely marginal because,  
 254 in contrast with what was observed for DIC (Havas et al., submitted), there is no correlation between the average  
 255 DOC concentration in the Mexican lakes and their salinity ( $R^2=0.47$ ,  $p=0.2$  for DOC and  $R^2=0.93$ ,  $p=5.8 \times 10^{-5}$  for  
 256 DIC). In the following discussion, we therefore explore the different patterns of DOC production and fate, in  
 257 relation to other environmental and biological variations, and how this can provide information about past DOC-  
 258 related perturbations of the C cycle.

259

### 260 5.1 Sources and fate of DOC

261 Due to their endorheic nature, the four lakes receive relatively little allochthonous OM (Alcocer et al., 2014b;  
 262 Havas et al., submitted). It is therefore possible to focus on DOC-related processes occurring within the water  
 263 column, particularly on autochthonous DOC primary production. Autochthonous DOC can form through higher-

264 rank OM degradation processes such as sloppy feeding by zooplankton, UV photolysis or bacterial and viral cell  
265 lysis (Lampert, 1978; Hessen, 1992; Bade et al., 2007; Thornton, 2014; Brailsford, 2019), as well as passive  
266 (leakage) or active (exudation) release by healthy cells (e.g. Baines and Pace, 1991; Hessen and Anderson, 2008;  
267 Thornton, 2014; Ivanovsky et al., 2020). Generally, this C release (whether “active” or “passive”) tends to be  
268 enhanced in nutrient-limited conditions because recently fixed C is in excess compared with other essential  
269 nutrients such as N or P (Hessen and Anderson, 2008; Morana et al., 2014; Ivanovsky et al., 2020). For oxygenic  
270 phototrophs, this is particularly true under high photosynthesis rates, because photorespiration bolsters the  
271 excretion of DOC (Renstrom-Kellner and Bergman, 1989). Oligotrophic conditions also tend to limit heterotrophic  
272 bacterial activity and thus preserve DOC stocks (Thornton, 2014; Dittmar, 2015). Both these production and  
273 preservation aspects are consistent with the trend of increasing DOC concentrations observed in the lakes, from  
274 the less oligotrophic La Alberca and La Preciosa (0.7 mM on average) to the more oligotrophic Alchichica  
275 (1.8 mM) and Atexcac (6.5 mM).

276

### 277 **5.1.1 DOC release by autotrophs**

278 In the four Mexican lakes, DOC concentration profiles exhibit one or several peaks occurring in both oxic and  
279 anoxic waters (Fig. 3). In La Alberca and La Preciosa, these peaks correlate with Chl *a* peaks, but not in the other  
280 two lakes. However, in Atexcac, a remarkable DOC peak (Fig. 3) occurs at the same depth as a peak of anoxygenic  
281 photosynthesis (Havas et al., submitted). These co-occurrences indicate that a large portion of DOC in these three  
282 lakes (at least at these depths) arises from the release of photosynthetic C fixed in excess. Phytoplankton in aerobic  
283 conditions generally releases dissolved organic matter by (i) an active “overflow mechanism” (DOM exudation)  
284 or (ii) passive diffusion through the cell membranes, but this remains to be shown for anoxygenic organisms. In  
285 the first case, DOM is actively released from the cells as a result of C fixation rates higher than growth and  
286 molecular synthesis rates (e.g. Baines and Pace, 1991). Hence, DOM exudation depends not only on the nature of  
287 primary producers (different taxa may display very different growth rates, photosynthetic efficiency, and exudation  
288 mechanisms), but also on environmental factors such as irradiance and nutrient availability (e.g. Otero and  
289 Vincenzini, 2003; Morana et al., 2014; Rao et al., 2021). Exudation of DOM may also serve “fitness-promoting  
290 purposes” such as storage, defense, or mutualistic goals (Bateson and Ward, 1988; Hessen and Anderson, 2008).  
291 In the case of passive diffusion, DOM release also depends on cell permeability and the outward DOC gradient,  
292 but is more directly related to the amount of phytoplankton biomass (e.g. Marañón et al., 2004). Thus, any new  
293 photosynthate production drives a steady DOM release rate, independent of environmental conditions to some  
294 extent (Marañón et al., 2004; Morana et al., 2014). The fact that La Alberca and La Preciosa have lower DOC but  
295 Chl *a* concentrations higher than Atexcac and Alchichica overall, suggests that DOC production does not directly  
296 relate to phytoplankton biomass and is not passively released. By contrast, active DOC release is supported by  
297 DOC isotope signatures. These tropical Mexican lakes correspond precisely to environmental contexts (high  
298 irradiance and oligotrophic freshwater bodies) where DOC exudation has been observed and is predicted (e.g.  
299 Baines and Pace, 1991; Morana et al., 2014; Thornton, 2014; Rao et al., 2021).

300 Release of DOC by primary producers can be characterized by the percentage of extracellular release (PER), which  
301 corresponds to the fraction of DOC over total (dissolved and particulate) OM primary production (e.g. Thornton  
302 et al., 2014). The PER is highly variable and averages about 13% of C biomass over a wide range of environments

303 (e.g. Baines and Pace, 1991; Thornton, 2014). Values as high as 99% have been reported (see Bertilsson and Jones,  
304 2003), showing that most of the fixed C can be released in the external aqueous media as DOC. At depths where  
305 oxygenic photosynthesis occurs, the DOC over total OC ratio averages approximately 95, 94, 99, and 85 % for La  
306 Alberca, La Preciosa, Atexcac, and Alchichica, respectively. Thus, although the PER was not directly measured,  
307 and some of the measured DOC may correspond to an older long-term DOC reservoir, the majority of DOC  
308 measured could represent a recent phytoplankton exudation.

309 The DOC peaks associated with primary production (mainly photosynthesis) are characterized by very positive  
310  $\Delta^{13}\text{C}_{\text{DOC-POC}}$  (from +3 to +18 ‰, Fig. 4). These signatures further support a primary origin of DOC as photosynthate  
311 release at these depths, rather than a secondary origin by OM degradation. Bacterial heterotrophy would generate  
312 smaller and rather negative  $\Delta^{13}\text{C}_{\text{DOC-POC}}$  (section 5.1.2. and references therein) and cell lysis or zooplankton sloppy  
313 feeding would also produce  $\delta^{13}\text{C}_{\text{DOC}}$  close to  $\delta^{13}\text{C}_{\text{POC}}$  values. Photo-degradation is unlikely to proceed at these  
314 depths and would not generate such positive fractionations (Chomicki, 2009). A switch from  $\text{CO}_{2(\text{aq})}$  to  $\text{HCO}_3^-$  as  
315 an inorganic C source (which differ by 10‰, e.g. Mook et al., 1974) would not adequately explain the deviation  
316 between  $\delta^{13}\text{C}_{\text{POC}}$  and  $\delta^{13}\text{C}_{\text{DOC}}$ . The isotopic enrichment of DOC molecules relative to POC must therefore have a  
317 different origin.

318 The  $^{13}\text{C}$ -enriched DOC could originate from photosynthetic organisms using a different C-fixation pathway,  
319 inducing a smaller isotopic fractionation (provided that these organisms contributed predominantly to the DOC  
320 rather than to the POC fraction). In La Alberca and Atexcac, anoxygenic phototrophic bacteria may release large  
321 amounts of DOC, especially under nutrient-limiting conditions (Ivanovsky et al., 2020). Unlike cyanobacteria or  
322 purple sulfur bacteria (PSB, anoxygenic phototrophs belonging to the Proteobacteria), which use the Calvin-  
323 Benson-Bassham pathway (CBB), green sulfur bacteria (GSB; another group of anoxygenic phototrophs belonging  
324 to the Chlorobi), use the reductive citric acid cycle or reverse tricarboxylic-TCA cycle, which tends to induce  
325 smaller isotopic fractionations (between ~ 3–13 ‰, Hayes, 2001). The DOC isotope signatures recorded in the  
326 hypolimnion of La Alberca ( $\epsilon_{\text{DOC-CO}_2} \approx -13.5 \pm 2$  ‰) agree well with fractionations found for this type of organism  
327 in laboratory cultures and in stratified water bodies (Posth et al., 2017). By contrast,  $\epsilon_{\text{DOC-CO}_2}$  signatures in the  
328 hypolimnion of Atexcac are higher ( $\epsilon_{\text{DOC-CO}_2} \approx 0$  ‰), and thus cannot be explained by the use of the reductive  
329 citric acid cycle C fixation pathway. Consistently, GSB were identified in La Alberca but not in Atexcac (Havas  
330 et al., submitted).

331 Phytoplankton blooms may specifically release isotopically heavy organic molecules. Carbohydrates could be  
332 preferentially released under nutrient-limiting conditions as they are devoid of N and P (Bertilsson and Jones,  
333 2003; Wetz and Wheeler, 2007; Thornton, 2014). Carbohydrates typically have a  $^{13}\text{C}$ -enriched (heavy) isotopic  
334 composition (Blair et al., 1985; Jiao et al., 2010; Close and Henderson, 2020). Considering the isotopic mass  
335 balance of cell specific organic compounds, this molecular hypothesis is insufficient to explain the full range of  
336  $\Delta^{13}\text{C}_{\text{DOC-POC}}$  variations measured in La Alberca and Atexcac (Hayes, 2001).

337 Alternatively, such enrichments require that DOC and DIC first accumulate in the cells. If DOC molecules were  
338 released as soon as they were produced, their isotopic composition would tend towards that of the biomass (i.e.  
339  $\delta^{13}\text{C}_{\text{POC}}$ , within the range of molecule-specific isotopic compositions), which is not the case. If DIC could freely  
340 exchange between inner and outer cell media, maximum “carboxylation-limited” fractionation (between ~ 18 and

341 30 ‰ depending on RuBisCO form, Thomas et al., 2019) would be expressed in all synthesized organic molecules,  
342 as represented in Fig. 5a (e.g. O’Leary, 1988; Descolas-Gros and Fontungne, 1990; Fry, 1996). This is also  
343 inconsistent with the DOC isotopic signatures (see  $\epsilon_{\text{DOC-CO}_2}$  in Table. 2).

344 Under the environmental conditions of the lakes studied (i.e. low  $\text{CO}_2$  relative to  $\text{HCO}_3^-$ , local planktonic  
345 competition for  $\text{CO}_2$ , and low nutrient availability), the activation of an intracellular DIC-concentrating mechanism  
346 (DIC-CM) is expected (Beardall et al., 1982; Burns and Beardall, 1987; Fogel and Cifuentes, 1993; Badger et al.,  
347 1998; Iñiguez et al., 2020). This mechanism is particularly relevant in oligotrophic aqueous media (Beardall et al.,  
348 1982), where  $\text{CO}_2$  diffusion is slower than in the air (O’Leary, 1988; Fogel and Cifuentes, 1993; Iñiguez et al.,  
349 2020). A DIC-CM has been proposed to reduce the efflux of DIC from the cells back to the extracellular solution.  
350 This internal DIC is eventually converted into organic biomass, thereby drawing the cell isotopic composition  
351 closer to that of  $\delta^{13}\text{C}_{\text{DIC}}$  (Fig. 5; Beardall et al., 1982; Fogel and Cifuentes, 1993; Werne and Hollander, 2004). As  
352 a conceptual model, we suggest that the activation of a DIC-CM could preserve a large  $\Delta^{13}\text{C}_{\text{POC-DIC}}$ , while  
353 generating an apparent fractionation between the DOC and POC molecules. The initially fixed OC would be  
354 discriminated against the heavy C isotopes, and incorporated into the cellular biomass (Fig. 5c, ‘ $t_i$ ’). In turn,  
355 following the overflow mechanism scenario, high photosynthetic rates (due to high irradiance and temperature,  
356 and high DIC despite low  $\text{CO}_2$ ) coupled with low population growth rates and organic molecule synthesis (due to  
357 limited abundances of P, N, and Fe), would result in the exudation of excess organic molecules with heavy  $\delta^{13}\text{C}_{\text{DOC}}$ ,  
358 as they are synthesized from residual internal DIC, which progressively becomes  $^{13}\text{C}$ -enriched (Fig. 5c, ‘ $t_{ii}$ ’). This  
359 process could explain the formation of DOC with  $\delta^{13}\text{C}$  very close to DIC/ $\text{CO}_2$  signatures as observed in Lake  
360 Atexcac. This suggests that oligotrophic conditions could be a determinant factor in the generation of significantly  
361 heavy  $\delta^{13}\text{C}_{\text{DOC}}$ , even more so if they are coupled to high irradiance. This also demonstrates that considerable  
362 isotopic variability can exist between these two organic C reservoirs.

363  
364 In summary, the unusual [DOC] and  $\delta^{13}\text{C}_{\text{DOC}}$  profiles in La Alberca, La Preciosa and Atexcac could be interpreted  
365 as mainly reflecting a prominent exudation of autochthonous C, fixed in excess by oxygenic and/or anoxygenic  
366 phototrophs in nutrient-poor and high-irradiance conditions. The striking  $^{13}\text{C}$ -rich signatures of these exudates are  
367 interpreted as reflecting either the activation of a DIC-CM by oxygenic and/or anoxygenic phototrophs or the  
368 fixation of C *via* the reductive citric acid cycle. We propose a conceptual model involving the DIC-CM, whereby  
369 oligotrophic and high irradiance contexts can lead to high  $\delta^{13}\text{C}_{\text{DOC}}$  compared to both  $\delta^{13}\text{C}_{\text{DIC}}$  and  $\delta^{13}\text{C}_{\text{POC}}$ .

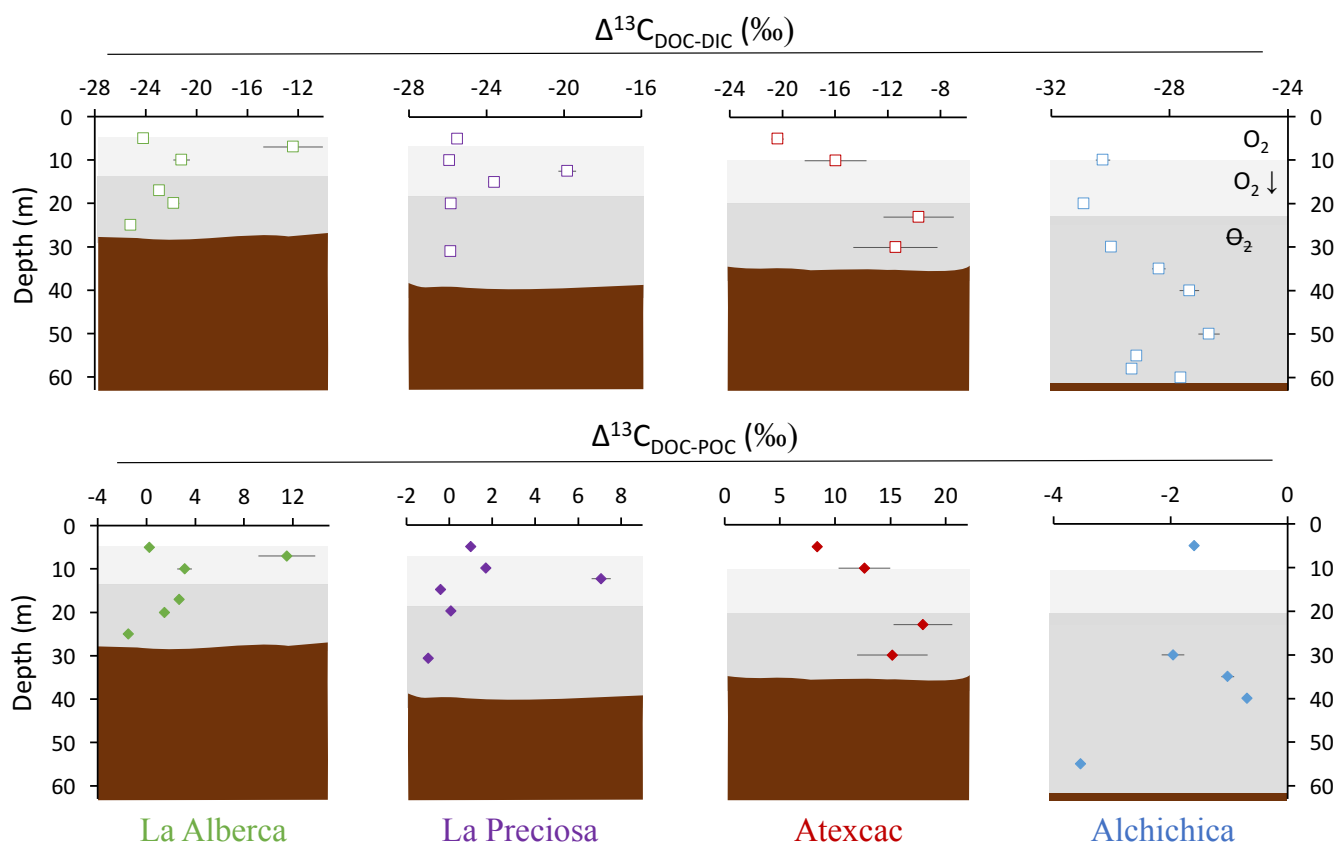
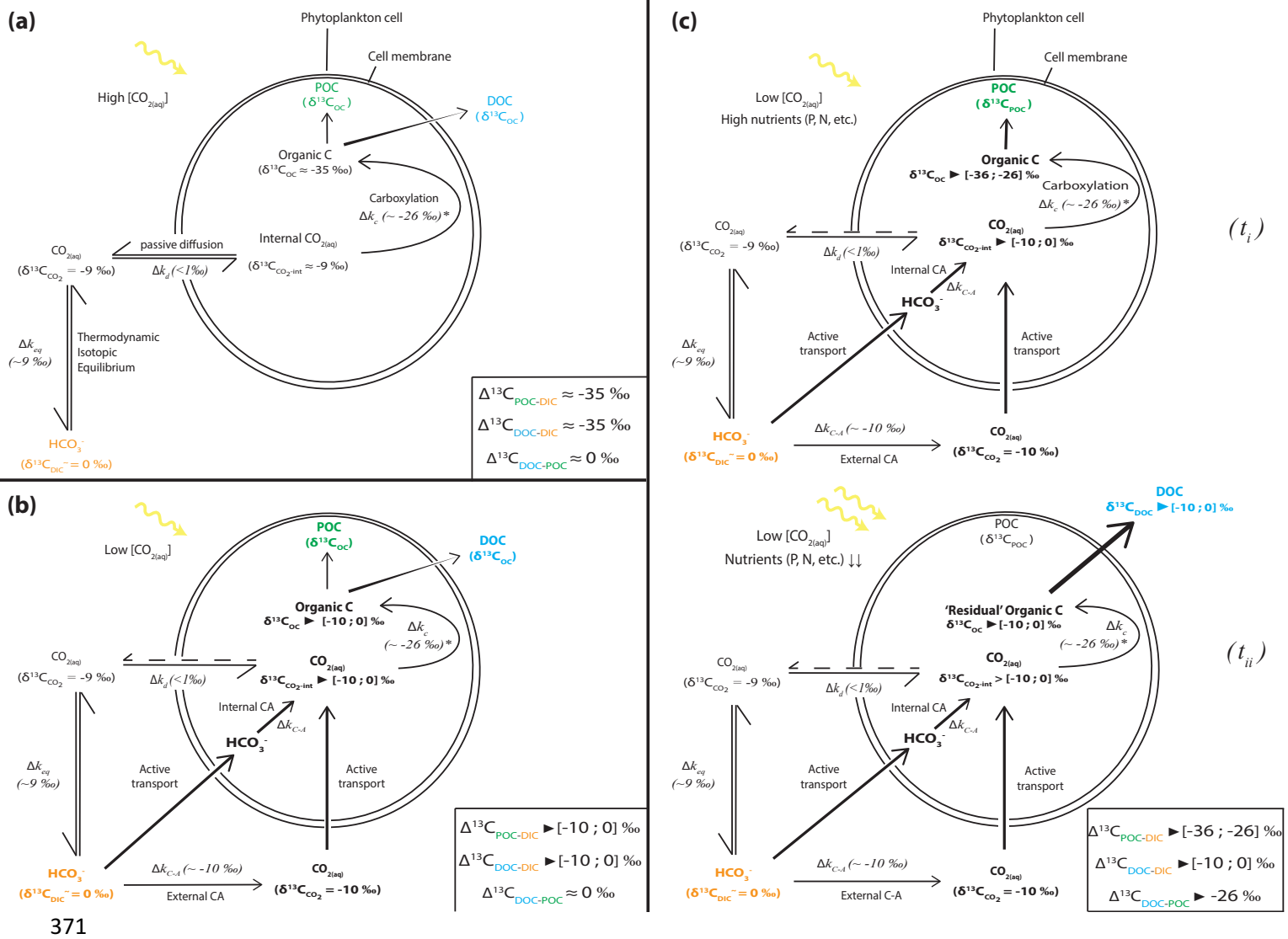


Figure 4. Vertical profiles of the difference in  $\delta^{13}\text{C}$  values of DOC and DIC (top) as well as DOC and POC (bottom) throughout the water columns of the four lakes (all expressed as  $\Delta^{13}\text{C}$  in ‰ vs. VPDB). POC and DIC data used in these calculations are from Havas et al. (submitted). In Alchichica,  $\delta^{13}\text{C}_{\text{DOC}}$  was not measured at 5 m and its value at 10 m was used in this calculation of  $\Delta^{13}\text{C}_{\text{DOC-POC}}$ . The white, gray, and dark gray shading is as in Fig. 2. The brown shading symbolizes the presence of sediment at the bottom of the water columns.



371

Figure 5. Schematic view of phytoplankton cells during autotrophic C fixation through different C supply strategies and associated apparent isotopic fractionation between DIC and POC/DOC and between DOC and POC. (a) Case where  $[CO_{2(aq)}]$  is high enough to allow for a DIC supply by passive  $CO_{2(aq)}$  diffusion through the cell membrane and  $CO_{2(aq)}$  is at equilibrium with other DIC species. Isotopic fractionation is maximum (minimum  $\delta^{13}C_{OC}$ ) because C fixation is limited by the carboxylation step. DOC is released following an in- to outward cell concentration gradient and has a similar composition to POC. (b) "Classic" view of C isotopic cycling resulting from active DIC transport within the cell because of low ambient  $[CO_{2(aq)}]$  (through a DIC-CM). Carbonic anhydrase (CA) catalyzes the conversion between  $HCO_3^-$  and  $CO_{2(aq)}$  inside or outside the cell with isotopic fractionation close to equilibrium fractionation ( $\sim 10\text{‰}$ ). While inward passive  $CO_{2(aq)}$  diffusion can still occur, the DIC-CM activation reduces the reverse diffusion, resulting in internal  $CO_{2(aq)}$  isotopic composition approaching that of the incoming DIC (depending on the fraction of internal  $CO_{2(aq)}$  leaving the cell). Acting as a "closed-system", most of the internal DIC is fixed as OC, and minimum isotopic fractionation is expressed for both POC and DOC. (c) Proposed model for C isotopic fractionation with active DIC transport including isotopic discrimination between POC and DOC.  $(t_i)$  Initially fixed C is isotopically depleted and incorporates the cell's biomass as long as there are sufficient nutrients to enable the synthesis of "complex" organic molecules.  $(t_{ii})$  In low nutrient conditions, but with high photosynthetic activity – subsequently fixed C is released out of the cell as DOC following the "overflow" hypothesis and inherits heavier isotopic compositions from the residual internal DIC. This leads to distinct POC and DOC isotopic signatures, with small fractionation between DOC and DIC, the amplitude of which will depend on the rate of  $CO_2$  backward diffusion, and the biomass C (POC) to released C (DOC) ratio.

### 372 5.1.2 OM partial degradation and DOC accumulation: the case of Lake Alchichica

373 From the previous discussion, it appears that the environmental conditions of the Mexican lakes favor substantial  
374 phytoplankton production of DOC. Alcocer et al. (2014a) proposed that an early spring cyanobacterial bloom in  
375 Lake Alchichica may favor the production of DOC in the epilimnion. However, at the time of sampling, the DOC  
376 reservoir in this lake was not correlated with any sizeable autotrophic activity at any depth. The large epilimnetic  
377 Chl a peak did not correlate with any changes in [DOC] or  $\delta^{13}\text{C}_{\text{DOC}}$  (Fig. 3). Compared with the other lakes, the  
378 geochemical conditions in which Chl a was produced in Alchichica may have been incompatible with the  
379 activation of a DIC-CM and significant DOC exudation. Alchichica had similar  $[\text{CO}_{2(\text{aq})}]$  to La Preciosa, but higher  
380 P and  $\text{NH}_4^+$  concentrations (Havas et al., submitted); La Alberca had higher P concentrations, but similar  $[\text{NH}_4^+]$   
381 and lower  $[\text{CO}_{2(\text{aq})}]$ . In contrast with measurements from 2013 (Alcocer et al., 2014a), we found a large increase  
382 in DOC in the middle of the anoxic hypolimnion of Alchichica, which did not correspond to any change in the  
383 DIC reservoir, unlike that observed for La Preciosa at 12.5 m and Atexcac at 23 m (Havas et al., submitted). At  
384 these depths, photosynthetic active radiation (PAR) is below 0.1% in Alchichica during the stratified season  
385 (Macek et al., 2020), which might not be sufficient to trigger major anoxygenic phytoplankton DOC release.

386 The DOC reservoir in Alchichica is characterized by a  $\delta^{13}\text{C}_{\text{DOC}}$  (and  $\Delta^{13}\text{C}_{\text{DOC-DIC}}$ ) lower than in the other lakes,  
387 systematically showing  $^{13}\text{C}$ -depleted signatures relative to POC (i.e.  $\delta^{13}\text{C}_{\text{DOC}} < \delta^{13}\text{C}_{\text{POC}}$ ; Fig. 4). Thus, if the DOC  
388 increase in the hypolimnion of Alchichica resulted from the release of photosynthetic OC, as in some of the other  
389 lakes, it was not associated with the same C isotope fractionation (e.g. if anoxygenic phototrophs did not  
390 concentrate intracellular DIC, cf. Fig. 5a). Some PSB have been identified but they only become abundant toward  
391 the end of the stratification (from July/August to December/January; Alcántara-Hernández et al., 2022; Iniesto et  
392 al., 2022).

393 Alternatively, the hypolimnetic DOC increase in Lake Alchichica may reflect the preservation and accumulation  
394 of DOM over the years, consistent with the higher [DOC] measured in 2019 than in the previous years (Alcocer  
395 et al., 2014a). While alteration of the DOC reservoir by UV-photolysis would induce positive isotopic fractionation  
396 (Chomicki, 2009), the slightly negative  $\Delta^{13}\text{C}_{\text{DOC-POC}}$  signatures support the possibility of DOC being mainly a  
397 recalcitrant residue of primary OM degradation by heterotrophic organisms (Alcocer et al., 2014a). The  
398 preferential consumption of labile  $^{13}\text{C}$ -enriched molecules by heterotrophic bacteria would leave the residual OM  
399 with more negative isotopic signatures (Williams and Gordon, 1970; Lehmann et al., 2002; Close and Henderson,  
400 2020). The DIC and POM data were also consistent with heterotrophic activity from the surface to the hypolimnion  
401 of Alchichica, by recording complementary decreasing and increasing  $\delta^{13}\text{C}$ , respectively, and a decreasing C:N  
402 ratio (Havas et al., submitted). Degradation by heterotrophic bacteria leaves more recalcitrant DOM in the water  
403 column, which tends to accumulate over longer periods of time (Ogawa et al., 2001; Jiao et al., 2010; Kawasaki et  
404 al., 2013). The DOM content is a balance between production by autotrophs and consumption by heterotrophs,  
405 especially in environments where both types of organisms compete for low-concentration nutrients (Dittmar,  
406 2015). If the DOC in Alchichica represents a long-term reservoir, its presence might favor the development of  
407 bacterial populations. A shift of the cyanobacterial DOC from the epilimnion toward the hypolimnion of  
408 Alchichica was described at the end of the spring (Alcocer et al., 2014a; 2022). Thus, part of the hypolimnetic  
409 DOC in Alchichica may originate from a phytoplankton release, as observed in the other lakes, but it was already  
410 partially degraded by heterotrophic bacteria at the time we sampled it. The deeper and darker anoxic waters of



411 Alchichica could help to better preserve this DOC from intense microbial and light degradation, hence allowing  
 412 its accumulation over time.

413 In conclusion, the DOC reservoir in Alchichica (notably in the hypolimnion) more likely represents an older, more  
 414 evolved DOM pool. The time required for its accumulation and long-term stability has not yet been evaluated.

415

416

417

Lake	Sample	$\Delta^{13}\text{C}_{\text{DOC-DIC}}$	$\Delta^{13}\text{C}_{\text{DOC-POC}}$	$\epsilon_{\text{DOC-CO}_2}$
		‰		‰
La Alberca de Los Espinos	Albesp 5m	-24.2	0.2	-14.8
	Albesp 7m	-12.4	11.5	-3.0
	Albesp 10m	-21.2	3.1	-11.6
	Albesp 17m	-22.9	2.7	-13.1
	Albesp 20m	-21.8	1.5	-12.2
	Albesp 25m	-25.2	-1.5	-15.9
La Preciosa	LP 5m	-25.5	1.0	-15.7
	LP 10m	-25.9	1.7	-16.0
	LP 12.5m	-19.8	7.1	-9.8
	LP 15m	-23.6	-0.4	-13.5
	LP 20m	-25.8	0.1	-15.7
	LP 31m	-25.8	-1.0	-15.7
Atexcac	ATX 5m	-20.4	8.4	-10.6
	ATX 10m	-16.0	12.6	-6.1
	ATX 23m	-9.7	17.9	0.6
	ATX 30m	-11.4	15.2	-1.2
Alchichica	AL 5m	ND.	-1.6	
	AL 10m	-30.3		-20.1
	AL 20m	-30.9		-20.5
	AL 30m	-30.0	-2.0	-19.5
	AL 35m	-28.4	-1.0	-17.9
	AL 40m	-27.3	-0.7	-16.8
	AL 50m	-26.7		-16.2
	AL 55m	-29.1	-3.5	-18.7
	AL 58m	-29.3		-18.8
AL 60m	-27.6		-17.1	

418

419 Table 2

420 Isotopic fractionation between DOC and DIC, and DOC and POC, where  $\Delta^{13}\text{C}_{x-y} = \delta^{13}\text{C}_x - \delta^{13}\text{C}_y$  is the apparent  
 421 fractionation and  $\epsilon$  is computed as the actual metabolic isotopic discrimination between  $\text{CO}_2$  and DOC. In  
 422 Alchichica,  $\delta^{13}\text{C}_{\text{DOC}}$  was not measured at 5 m, and its value at 10 m was used in this calculation of  $\Delta^{13}\text{C}_{\text{DOC-POC}}$ . The  
 423 full chemistry at depths 35 and 58 m was not determined, thus the calculation of  $\delta^{13}\text{C}_{\text{CO}_2}$  for these samples is  
 424 based on the composition of samples above and below. Isotopic data for DIC, POC, and  $\text{CO}_2$  are from Havas et al.  
 425 (submitted).

426

427

428

429 **5.2 DOC analysis provides deeper insights into planktonic cell functioning and water column C cycle**  
430 **dynamics than POC or DIC analyses**

431 The depth profiles of DOC concentration and isotope composition differ significantly from those of POC. Notably  
432 in La Preciosa, the photosynthetic DOC production (+1.5 mM) at the Chl a peak depth matches the decrease in  
433 DIC (- 2 mM), while there was no change in [POC] or  $\delta^{13}\text{C}_{\text{POC}}$  (Havas et al., submitted). Just below, at 15 m depth,  
434  $\delta^{13}\text{C}_{\text{POC}}$  exhibited a marked increase (+3.6 ‰) interpreted as reflecting heterotrophic activity (Havas et al.,  
435 submitted). It is likely explained by the production of DOC with heavier isotope compositions between 12.5 and  
436 15 m depth, and its consumption by heterotrophic organisms (as seen with  $\Delta^{13}\text{C}_{\text{DOC-POC}} \approx 0$ ). In La Alberca, the  
437 peaks of oxygenic and anoxygenic photosynthesis clearly stand out from DOC concentrations (+ 0.5/1.5 mM), but  
438 not from POC concentrations (+ <0.03 mM), while the DIC geochemical signatures reflected the influence of OC  
439 respiration, sediment-associated methanogenesis, and possible volcanic degassing at the bottom of the lake (Havas  
440 et al., submitted). In Atexcac, anoxygenic photosynthesis is clearly evidenced by [DOC] and  $\delta^{13}\text{C}_{\text{DOC}}$  data (see  
441 5.1.1), but is not recorded by the POC reservoir (a decrease of 0.03 mM at this depth) and not as distinctively by  
442 the DIC reservoir (a decrease of ~ 2 mM; Havas et al., submitted). It implies that recently fixed OC is quickly  
443 released out of the cells as DOC, transferring most C from DIC to DOC, rather than POC, which is therefore an  
444 incomplete archive of the biogeochemical reactions occurring in water columns. The isotopic analysis of DIC, and  
445 by extension of authigenic carbonates, especially in alkaline-buffered waters, might not be sensitive enough to  
446 faithfully record all environmental and biological changes.

447 The  $\delta^{13}\text{C}_{\text{DOC}}$  recorded in La Alberca, La Preciosa, and Atexcac present peculiar heavy signatures, which provide  
448 strong constraints on planktons intra-cellular functioning and their use of C. These signatures may arise from the  
449 activation of a DIC-CM or from a specific metabolism or C-fixation pathway. By contrast, the use of a DIC-CM  
450 is poorly captured by  $\delta^{13}\text{C}_{\text{POC}}$ , although recognition of active DIC uptake has often been based on this signal (by  
451 reduced isotopic fractionation with DIC; e.g. Beardall et al., 1982; Erez et al., 1998; Riebesell et al., 2000). Most  
452 interestingly, intra-cellular amorphous Ca-carbonates (iACC) are formed in some of the cyanobacteria from  
453 Alchichica microbialites, possibly due to supersaturated intra-cell media following active DIC uptake through a  
454 DIC-CM (Couradeau et al., 2012; Benzerara et al., 2014). While the link between DIC-CM and iACC still needs  
455 to be demonstrated (Benzerara et al., 2014), the active use of DIC-CMs in Mexican lakes is independently  
456 supported by the DOC isotopic signature.

457 In summary, the analysis of DOC concentrations and isotope compositions showed that most of the autochthonous  
458 C fixation ends up in the DOC reservoir, thus highlighting important features of the lakes and their C cycle that  
459 were not evidenced by POC and DIC analyses alone, notably the activation of a DIC-CM and a better description  
460 of the planktonic diversity. In the future, it will be interesting to couple the present analyses with deeper molecular  
461 and compound-specific isotopic analyses of DOM (Wagner et al., 2020).

462

463

464

### 465 **5.3 Implications for the hypothesis of a large DOC reservoir controlling past carbon cycling**

466 In these Mexican lakes, the DOC concentrations (from 0.6 to 6.5 mM on average) are between 14 and 160 times  
467 higher than the POC concentrations. The DOC represents from 5 to 16% of the total C measured in the four lakes.  
468 In comparison, it remains under 0.3 mM in large-scale anoxic basins such as the Black Sea (Ducklow et al., 2007).  
469 In the modern ocean, DOC is also the main organic pool but its concentration rarely exceeds 0.08 mM (Hansell,  
470 2013). Thus, the DOC pools of these lakes is much larger than in the modern ocean and can be used to draw  
471 comparisons with studies invoking past occurrences of oceanic carbon cycles dominated by vast DOC reservoirs  
472 (e.g. Rothman et al., 2003; Sexton et al., 2011).

473

#### 474 **5.3.1 Eocene carbon isotope excursions (CIEs)**

475 Ventilation/oxidation cycles of a large deep ocean DOC reservoir have been inferred to explain carbonate isotopic  
476 records of successive warming events through the Eocene (Sexton et al., 2011). In this scenario, the release of  
477 carbon dioxide into the ocean/atmosphere system following DOC oxidation would trigger both the precipitation  
478 of low  $\delta^{13}\text{C}$  carbonates and an increase of the atmospheric greenhouse gas content. The size of this DOC reservoir  
479 should have been at least 1600 PgC (about twice the size of the modern ocean DOC reservoir) to account for a 2–  
480 4°C increase in deep ocean temperatures (Sexton et al., 2011). However, the main counter-argument to this  
481 hypothesis is that the buildup of such a DOC reservoir at modern DOC production rates implies sustained deep  
482 ocean anoxia over several hundred thousand years, while independent geochemical proxies do not support the  
483 persistence of such anoxic conditions (Rigwell and Arndt, 2015). Our study suggests, albeit at a different scale,  
484 that this kinetic argument may be weak. In these Mexican lakes, the lowest recorded [DOC] is 260  $\mu\text{M}$  (Table 1),  
485 which is about 6 times the deep modern ocean concentration ( $\sim 45 \mu\text{M}$ ; Hansell, 2013). Yet the entire water  
486 columns of these lakes down to the surficial sediments are seasonally mixed with di-oxygen, showing that high  
487 [DOC] (notably in Alchichica, which likely harbors a “long-term” DOC reservoir) can be achieved despite frequent  
488 oxidative conditions. The oxidation of only half of the DOC in the lakes would generate average  $\delta^{13}\text{C}_{\text{DIC}}$  deviations  
489 between -0.6 and -1 ‰, corresponding to the C isotope excursion magnitudes described by Sexton et al. (2011).

490 Similarly, deep anoxic waters in the Black Sea hold about 3 times the amount of DOC found in the modern deep  
491 open ocean (Ducklow et al., 2007; Sexton et al., 2011; Dittmar, 2015). In the Black Sea and in the Mexican lakes,  
492 low nutrient availability may limit sulfate-reduction despite high sulfate and labile organic matter concentrations,  
493 thus favoring DOM preservation and accumulation (Dittmar, 2015 and references therein). Margolin et al. (2016)  
494 argued that substantial DOM is maintained in the Black Sea by large terrigenous inputs only. Our study attests the  
495 possibility for “autochthonous systems” to reach DOC concentrations well above what is found in the Black Sea,  
496 without requiring terrigenous inputs. Therefore, it supports the hypothesis that the buildup of a large DOC reservoir  
497 may have influenced the carbonate isotopic record of Eocene warming events. Nonetheless, it remains to be proven  
498 how this could apply to larger oceanic-type basins, with more variable environmental conditions (e.g. tropical vs.  
499 polar latitudes), greater diversity of eukaryotic heterotrophs (in Phanerozoic oceans), and more active water  
500 currents and ventilation processes. A better characterization of the molecular composition of DOM in the Mexican  
501 lakes will help to understand how it can accumulate over time and refine the suggested analogy with Phanerozoic  
502 CIEs. Furthermore, investigating the paleo-ecology and -geography of the CIE time period will also help to  
503 constrain the potential applicability of a large DOC hypothesis (Sexton et al., 2011).

### 504 5.3.2 Neoproterozoic carbon isotope excursions (CIEs)

505 The presence of a large oceanic DOC reservoir has also been used to account for the Neoproterozoic C isotope  
506 record, where carbonates show  $\delta^{13}\text{C}$  negative excursions of more than 10‰ over tens of Ma (Rothman et al., 2003;  
507 Fike et al., 2006; Swanson-Hysell et al., 2010; Tziperman et al., 2011). Once again, this hypothesis has been  
508 questioned because of (i) the oversized DOC reservoir (10 times the contemporaneous DIC, i.e.,  $10^2$  to  $10^3$  times  
509 that of modern DOC) and (ii) the amount of oxidants required to generate such a sustained DOC oxidation process  
510 (see Ridgwell and Arndt, 2015). Recent studies offered potential explanations for this latter issue showing that  
511 pulses of continental weathering and an associated increase of sulfate supply would have provided sufficient  
512 oxidant (Shields et al., 2019; Chen et al., 2022), while lateral heterogeneity of the carbonate geochemical signatures  
513 – with a restricted record of the CIEs on the continental shelves – would require lower amounts of oxidant (Li et  
514 al., 2017; Shi et al., 2017).

515 Critically though, direct evidence for the existence of such high oceanic DOC levels in the past remains scarce (Li  
516 et al., 2017), although multiple studies have built on the Neoproterozoic large DOC scenario (e.g. Sperling et al.,  
517 2011; Cañadas et al., 2022). Purported high oceanic DOC concentrations during the Ediacaran period have been  
518 estimated from the Ge/Si ratio of diagenetic chert nodules (Xing et al., 2022) but they reflect the sediments  
519 porewater geochemistry and remain difficult to directly relate to the ocean water itself. Besides, some modeling  
520 approaches have suggested that DOC abundance in the past Earth's oceans could not have markedly differed from  
521 today's values (Fakraee et al., 2021).

522 Modern analogous systems such as the Black Sea or Mexican lakes studied here support the possibility of greater  
523 DOC accumulation in anoxic waters (Ducklow et al., 2007), but only to levels substantially lower than those  
524 required to account for the Neoproterozoic CIEs (minimum concentrations estimated between 25 and 100 mM;  
525 Ridgwell and Arndt, 2015). One could argue that the development of larger DOC pools in the three Mexican lakes  
526 from the SOB is hindered by relatively large sulfate reservoirs (especially in Alchichica ~10 mM). However, we  
527 notice that La Alberca does not show a larger DOC reservoir despite having the lowest oxidant availability (both  
528 oxygen- and sulfate-free at depth) and being the only one of the four lakes to present isotopic signatures associated  
529 with methanogenesis (Havas et al., submitted). Furthermore, the Mexican lakes are seasonally oxidized, which  
530 could consume part of their DOC reservoir. However, the Black Sea is permanently stratified and shows even  
531 lower [DOC], suggesting that DOC production might be the primary control on DOC concentration over DOC  
532 oxidation. The processes of DOC production and accumulation in the Neoproterozoic ocean could have been less  
533 efficient than today (Fakraee et al. 2021). Nonetheless, an important limit to the analogy between modern  
534 analogues and the Precambrian oceans is the difference in time over which DOC could have accumulated in both  
535 environments (Ridgwell and Arndt, 2015). One could expect the formation of such a large autochthonous DOC  
536 reservoir to increase the ocean inorganic C isotope composition, by mass balance. However, from  $\delta^{13}\text{C}_{\text{Carb}}$  data  
537 compilation (e.g. Fike et al., 2006; Saltzman and Thomas, 2012; Li et al., 2017), we see that there are no positive  
538 increases of  $\delta^{13}\text{C}_{\text{Carb}}$  at the magnitude of the negative CIEs tens to hundreds of million years before the  
539 Neoproterozoic CIEs. Thus, even if the “oxidant paradox” may have found satisfactory explanations, the origin of  
540 the massive DOC reservoir required to generate these excursions still remains to be elucidated (Jiang et al., 2010;  
541 Lu et al., 2013; Li et al., 2017).

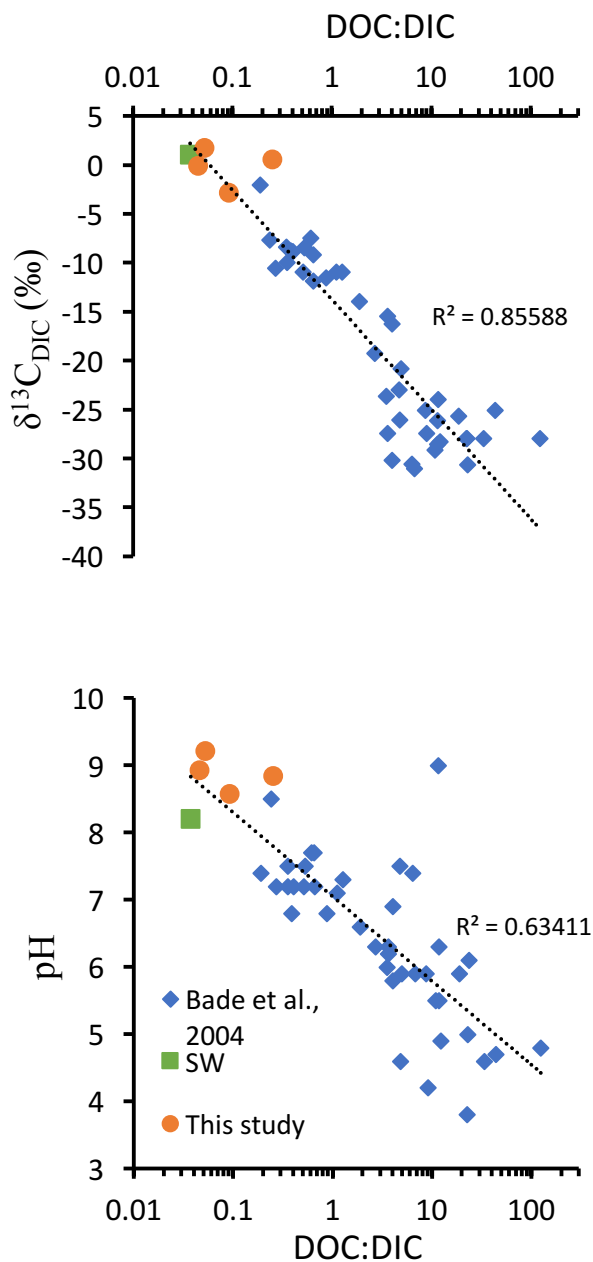


Figure 6. DOC:DIC ratios, pH and  $\delta^{13}\text{C}_{\text{DIC}}$  values from different lakes compiled from Bade et al. (2004) and the four Mexican lakes from Havas et al. (submitted), as well as modern surface ocean values (from Kroopnick, 1985; Zeebe and Wolf-Gladrow, 2009 and Hansell, 2013).

Top:  $\delta^{13}\text{C}_{\text{DIC}}$  as a function of DOC:DIC ratio represented with a logarithmic abscissa scale and logarithmic trend line which combines the three datasets.

Bottom: pH as a function of DOC:DIC ratio, with a logarithmic abscissa scale and logarithmic trend line which combines the three datasets.

542

543

544

545 In the alkaline lakes studied, oxidation of the DOC reservoir would generate a maximum  $\delta^{13}\text{C}_{\text{DIC}}$  deviation of -  
 546 2 ‰, in La Alberca de los Espinos, which has the lowest alkalinity. The other lakes  $\delta^{13}\text{C}_{\text{DIC}}$  are less impacted,  
 547 notably because they are largely buffered by high DIC content (Havas et al., submitted). Bade et al. (2004) showed  
 548 that modern low alkalinity/low pH lakes generally show more negative  $\delta^{13}\text{C}_{\text{DIC}}$  (down to  $\sim -30$  ‰), partly due to a  
 549 higher responsiveness of the  $\delta^{13}\text{C}_{\text{DIC}}$  to remineralization of OM and especially DOC. Compiling our data with  
 550 those of Bade et al. (2004), we consistently show a clear negative trend of  $\delta^{13}\text{C}_{\text{DIC}}$  with an increasing DOC:DIC  
 551 ratio over a broad range of lacustrine DOC and DIC concentrations (Fig. 6). This trend also matches modern ocean  
 552 values (Fig. 6). These observations are consistent with the inference that systems where  $\text{DOC:DIC} \gg 1$  should  
 553 drive  $\delta^{13}\text{C}_{\text{DIC}}$  to very negative values (Rothman et al., 2003). However, in modern environments, the biomass is

554 largely influenced by aerobic heterotrophs and high DOC:DIC waters usually lean toward acidic pHs (Fig. 6; Bade  
555 et al., 2004), at which carbonate precipitation is prevented. Instead, in anoxic waters, remineralization of OM  
556 through sulfate- or iron-reduction generates alkalinity (e.g. Tziperman et al., 2011). Hence, environmental  
557 conditions where DOC:DIC  $\gg$  1 might be inconsistent with large carbonate deposits unless they are associated  
558 with anaerobic remineralization. This further supports the hypothesis that negative  $\delta^{13}\text{C}_{\text{Carb}}$  excursions of the  
559 Ediacaran were triggered by continental sulfate addition to the ocean (Li et al., 2017; Shields et al., 2019; Chen et  
560 al., 2022), but following the oxidation of DOC by anaerobic (e.g. sulfate reduction) rather than aerobic (e.g. by  
561 free oxygen) pathways. At the same time, additional DOC inputs (e.g. terrigenous) might be necessary to reach  
562 the required high DOC conditions allowing the Neoproterozoic CIEs. This echoes previous suggestions of  
563 “Neoproterozoic greening”, referring to a phase of biological land colonization, although evidence for this  
564 phenomenon currently remains equivocal (Lenton and Daines, 2017). While a concomitant supply of sulfate and  
565 DOC *via* rivers may cause – at least – a partial oxidation of DOC, it would still result in a  $^{13}\text{C}$ -depleted source of  
566 alkalinity to the coastal environments.

567 The inferences from Fig. 6 also foster the scenario proposed by Tziperman et al. (2011) where the anaerobic  
568 respiration of a large DOM production leads to the sequestration of newly produced C in carbonates – with very  
569 negative  $\delta^{13}\text{C}$  – and thereby to the drawdown of atmospheric  $\text{pCO}_2$  and the initiation of Cryogenian glaciations.  
570 We therefore suggest that the climatic feedbacks associated with the negative Neoproterozoic CIEs have been  
571 controlled by the total amount and balance between different DOC sources (autochthonous vs. allochthonous), and  
572 different oxidation pathways (e.g. via  $\text{O}_2$  vs.  $\text{SO}_4^{2-}$ ).

573 In summary, Neoproterozoic carbonate carbon isotope excursions likely require DOC and DIC pools to be spatially  
574 decoupled (e.g. through terrestrial DOM inputs), which suggests that DOC was not necessarily larger than DIC in  
575 the entire ocean. The analogues studied here further support that the Neoproterozoic CIEs recorded in carbonates  
576 should have occurred following DOC oxidation through anaerobic rather than aerobic pathways.

577

## 578 6. CONCLUSIONS AND SUMMARY

579 Based on its concentration and isotopic signatures, we characterized the nature and role of the DOC reservoir  
580 within the C cycle of four stratified alkaline crater lakes, in comparison with previously described DIC and POC  
581 data. Despite similar contexts, the DOC reservoirs of the four lakes show considerable variability, driven by  
582 environmental and ecological differences, as summarized below:

- 583 - The DOC is the largest OC reservoir in the water column of the studied lakes (> 90%). Its concentration  
584 and isotopic composition provide novel information about the C cycle of these stratified water bodies. In  
585 each of the four lakes, diverse photosynthetic planktonic communities release greater or smaller amounts  
586 of DOC, depending strongly on environmental factors such as nutrient and DIC availability, and transfer  
587 most of the inorganic C to DOC rather than POC.
- 588 - This process is marked by very heavy and distinct isotopic signatures of DOC compared with POC. They  
589 reflect different metabolism/C fixation pathways and/or the activity of a DIC-CM coupled with an  
590 overflow mechanism (i.e. DOM exudation), which could be active for both oxygenic and anoxygenic

591 phototrophs, and for which we propose a novel isotopic model of cell carbon cycling, integrating DOC  
592 molecules.

593 - The DOC reservoir in one of the lakes was not characterized by this release process, but rather by partial  
594 degradation and accumulation in anoxic waters, associated with more negative isotopic signatures.

595 - Our results bring further constraints on the environmental conditions under which autochthonous DOM  
596 can accumulate in anoxic water bodies, providing boundary conditions to the large DOC reservoir  
597 scenarios. This study of modern redox-stratified analogues supports the idea that a large oceanic DOC  
598 reservoir may have generated the record of successive C isotope excursions during the Eocene. Our study  
599 suggests, however, that the Neoproterozoic large DOC hypothesis and its record in carbonates as negative  
600 CIEs would only have been possible if external DOC sources largely contributed, and if DOC oxidation  
601 occurred *via* anaerobic pathways.

602

### 603 **Author Contributions**

604 RH and CT designed the study in a project directed by PLG, KB and CT. CT, MI, DJ, DM, RT, PLG and KB  
605 collected the samples on the field. RH carried out the measurements for C data; DJ the physico-chemical parameter  
606 probe measurements and EM provided data for trace and major elements. RH and CT analyzed the data. RH wrote  
607 the manuscript with important contributions of all co-authors.

608

### 609 **Competing Interests**

610 The authors declare that they have no conflict of interest.

611

### 612 **Disclaimer**

613

### 614 **Acknowledgements**

615 This work was supported by Agence Nationale de la Recherche (France; ANR Microbialites, grant number ANR-  
616 18-CE02-0013-02). The authors thank Anne-Lise Santoni, Elodie Cognard, Théophile Cocquerez and the GISMO  
617 platform (Biogéosciences, University Bourgogne Franche-Comté, UMR CNRS 6282, France). We thank Céline  
618 Liorzou and Bleuenn Guéguen for the analyses at the Pôle Spectrométrie Océan (Laboratoire Géo-Océan, Brest,  
619 France) and Laure Cordier for ion chromatography analyses at IPGP (France). We thank Nelly Assayag and Pierre  
620 Cadeau for their help on the AP 2003 at IPGP.

621

### 622 **References**

623 Alcántara-Hernández, R.J., Macek, M., Torres-Huesca, J., Arellano-Posadas, J., Valdespino-Castillo,  
624 P.M., 2022. Bacterioplankton, in: Alcocer, J. (Ed.), Lake Alchichica Limnology: The Uniqueness of a  
625 Tropical Maar Lake. Springer International Publishing, Cham, pp. 183–196.

626 [https://doi.org/10.1007/978-3-030-79096-7\\_11](https://doi.org/10.1007/978-3-030-79096-7_11)

627 Alcocer, J., Guzmán-Arias, A., Oseguera, L.A., Escobar, E., 2014a. Dinámica del carbono orgánico  
628 disuelto y particulado asociados al florecimiento de *Nodularia spumigena* en un lago tropical  
629 oligotrófico. *Programma Mex. Carbono* 13.

630 Alcocer, J., Ruiz-Fernández, A.C., Escobar, E., Pérez-Bernal, L.H., Oseguera, L.A., Ardiles-Gloria, V.,  
631 2014b. Deposition, burial and sequestration of carbon in an oligotrophic, tropical lake. *J. Limnol.* 73.  
632 <https://doi.org/10.4081/jlimnol.2014.783>

633 Anderson, N.John., Stedmon, C.A., 2007. The effect of evapoconcentration on dissolved organic  
634 carbon concentration and quality in lakes of SW Greenland. *Freshw. Biol.* 52, 280–289.  
635 <https://doi.org/10.1111/j.1365-2427.2006.01688.x>

636 Armienta, M.A., Vilaclara, G., De la Cruz-Reyna, S., Ramos, S., Cenicerros, N., Cruz, O., Aguayo, A.,  
637 Arcega-Cabrera, F., 2008. Water chemistry of lakes related to active and inactive Mexican volcanoes.  
638 *J. Volcanol. Geotherm. Res.* 178, 249–258. <https://doi.org/10.1016/j.jvolgeores.2008.06.019>

639 Bade, D.L., Carpenter, S.R., Cole, J.J., Hanson, P.C., Hesslein, R.H., 2004. Controls of  $\delta^{13}\text{C}$ -DIC in lakes:  
640 Geochemistry, lake metabolism, and morphometry. *Limnol. Oceanogr.* 49, 1160–1172.  
641 <https://doi.org/10.4319/lo.2004.49.4.1160>

642 Bade, D.L., Carpenter, S.R., Cole, J.J., Pace, M.L., Kritzberg, E., Van de Bogert, M.C., Cory, R.M.,  
643 McKnight, D.M., 2007. Sources and fates of dissolved organic carbon in lakes as determined by  
644 whole-lake carbon isotope additions. *Biogeochemistry* 84, 115–129. [https://doi.org/10.1007/s10533-](https://doi.org/10.1007/s10533-006-9013-y)  
645 [006-9013-y](https://doi.org/10.1007/s10533-006-9013-y)

646 Badger, M.R., Andrews, T.J., Whitney, S.M., Ludwig, M., Yellowlees, D.C., Leggat, W., Price, G.D.,  
647 1998. The diversity and coevolution of Rubisco, plastids, pyrenoids, and chloroplast-based CO<sub>2</sub>-  
648 concentrating mechanisms in algae 76, 20.

649 Baines, S.B., Pace, M.L., 1991. The production of dissolved organic matter by phytoplankton and its  
650 importance to bacteria: Patterns across marine and freshwater systems. *Limnol. Oceanogr.* 36, 1078–  
651 1090. <https://doi.org/10.4319/lo.1991.36.6.1078>

652 Barber, A., Sirois, M., Chaillou, G., Gélinas, Y., 2017. Stable isotope analysis of dissolved organic  
653 carbon in Canada's eastern coastal waters: Stable isotope analysis of DOC. *Limnol. Oceanogr.* 62,  
654 S71–S84. <https://doi.org/10.1002/lno.10666>

655 Bateson, M.M., Ward, D.M., 1988. Photoexcretion and Fate of Glycolate in a Hot Spring  
656 Cyanobacterial Mat. *Appl. Environ. Microbiol.* 54, 1738–1743.  
657 <https://doi.org/10.1128/aem.54.7.1738-1743.1988>

658 Beardall, J., Griffiths, H., Raven, J.A., 1982. Carbon Isotope Discrimination and the CO<sub>2</sub> Accumulating  
659 Mechanism in *Chlorella emersonii*. *J. Exp. Bot.* 33, 729–737. <https://doi.org/10.1093/jxb/33.4.729>

660 Beaupré, S.R., 2015. The Carbon Isotopic Composition of Marine DOC, in: *Biogeochemistry of Marine*  
661 *Dissolved Organic Matter*. Elsevier, pp. 335–368. [https://doi.org/10.1016/B978-0-12-405940-](https://doi.org/10.1016/B978-0-12-405940-5.00006-6)  
662 [5.00006-6](https://doi.org/10.1016/B978-0-12-405940-5.00006-6)

663 Benzerara, K., Skouri-Panet, F., Li, J., Féraud, C., Gugger, M., Laurent, T., Couradeau, E., Ragon, M.,  
664 Cosmidis, J., Menguy, N., Margaret-Oliver, I., Tavera, R., López-García, P., Moreira, D., 2014.  
665 Intracellular Ca-carbonate biomineralization is widespread in cyanobacteria. *Proc. Natl. Acad. Sci.*  
666 111, 10933–10938. <https://doi.org/10.1073/pnas.1403510111>

667 Bertilsson, S., Jones, J.B., 2003. Supply of Dissolved Organic Matter to Aquatic Ecosystems:  
668 Autochthonous Sources, in: Findlay, S.E.G., Sinsabaugh, R.L. (Eds.), *Aquatic Ecosystems, Aquatic*  
669 *Ecology*. Academic Press, Burlington, pp. 3–24. <https://doi.org/10.1016/B978-012256371-3/50002-0>



670 Blair, N., Leu, A., Muñoz, E., Olsen, J., Kwong, E., Des Marais, D., 1985. Carbon isotopic fractionation  
671 in heterotrophic microbial metabolism. *Appl. Environ. Microbiol.* 50, 996–1001.  
672 <https://doi.org/10.1128/aem.50.4.996-1001.1985>

673 Brailsford, F.L., 2019. Dissolved organic matter (DOM) in freshwater ecosystems. Bangor University.

674 Burns, B.D., Beardall, J., 1987. Utilization of inorganic carbon by marine microalgae. *J. Exp. Mar. Biol.*  
675 *Ecol.* 107, 75–86. [https://doi.org/10.1016/0022-0981\(87\)90125-0](https://doi.org/10.1016/0022-0981(87)90125-0)

676 Cadeau, P., Jézéquel, D., Lebourlanger, C., Fouilland, E., Le Floc'h, E., Chaduteau, C., Milesi, V.,  
677 Guélard, J., Sarazin, G., Katz, A., d'Amore, S., Bernard, C., Ader, M., 2020. Carbon isotope evidence for  
678 large methane emissions to the Proterozoic atmosphere. *Sci. Rep.* 10, 18186.  
679 <https://doi.org/10.1038/s41598-020-75100-x>

680 Cañadas, F., Papineau, D., Leng, M.J., Li, C., 2022. Extensive primary production promoted the  
681 recovery of the Ediacaran Shuram excursion. *Nat. Commun.* 13, 148.  
682 <https://doi.org/10.1038/s41467-021-27812-5>

683 Carlson, C.A., Hansell, D.A., 2015. DOM Sources, Sinks, Reactivity, and Budgets, in: *Biogeochemistry*  
684 *of Marine Dissolved Organic Matter*. Elsevier, pp. 65–126. <https://doi.org/10.1016/B978-0-12-405940-5.00003-0>

686 Carrasco-Núñez, G., Ort, M.H., Romero, C., 2007. Evolution and hydrological conditions of a maar  
687 volcano (Atexcac crater, Eastern Mexico). *J. Volcanol. Geotherm. Res.* 159, 179–197.  
688 <https://doi.org/10.1016/j.jvolgeores.2006.07.001>

689 Cawley, K.M., Ding, Y., Fourqrean, J., Jaffé, R., 2012. Characterising the sources and fate of dissolved  
690 organic matter in Shark Bay, Australia: a preliminary study using optical properties and stable carbon  
691 isotopes. *Mar. Freshw. Res.* 63, 1098. <https://doi.org/10.1071/MF12028>

692 Chako Tchamabé, B., Carrasco-Núñez, G., Miggins, D.P., Németh, K., 2020. Late Pleistocene to  
693 Holocene activity of Alchichica maar volcano, eastern Trans-Mexican Volcanic Belt. *J. South Am. Earth*  
694 *Sci.* 97, 102404. <https://doi.org/10.1016/j.jsames.2019.102404>

695 Chen, B., Hu, C., Mills, B.J.W., He, T., Andersen, M.B., Chen, X., Liu, P., Lu, M., Newton, R.J., Poulton,  
696 S.W., Shields, G.A., Zhu, M., 2022. A short-lived oxidation event during the early Ediacaran and  
697 delayed oxygenation of the Proterozoic ocean. *Earth Planet. Sci. Lett.* 577, 117274.  
698 <https://doi.org/10.1016/j.epsl.2021.117274>

699 Chomicki, K., 2009. The use of stable carbon and oxygen isotopes to examine the fate of dissolved  
700 organic matter in two small, oligotrophic Canadian Shield lakes. University of Waterloo.

701 Close, H.G., Henderson, L.C., 2020. Open-Ocean Minima in  $\delta^{13}\text{C}$  Values of Particulate Organic Carbon  
702 in the Lower Euphotic Zone. *Front. Mar. Sci.* 7, 540165. <https://doi.org/10.3389/fmars.2020.540165>

703 Couradeau, E., Benzerara, K., Gérard, E., Moreira, D., Bernard, S., Brown, G.E., López-García, P., 2012.  
704 An Early-Branching Microbialite Cyanobacterium Forms Intracellular Carbonates. *Science* 336, 459–  
705 462. <https://doi.org/10.1126/science.1216171>

706 Crowe, S.A., Katsev, S., Leslie, K., Sturm, A., Magen, C., Nomosatryo, S., Pack, M.A., Kessler, J.D.,  
707 Reeburgh, W.S., Roberts, J.A., González, L., Douglas Haffner, G., Mucci, A., Sundby, B., Fowle, D.A.,  
708 2011. The methane cycle in ferruginous Lake Matano: Methane cycle in ferruginous Lake Matano.  
709 *Geobiology* 9, 61–78. <https://doi.org/10.1111/j.1472-4669.2010.00257.x>

710 Descolas-Gros, C., Fontungne, M., 1990. Stable carbon isotope fractionation by marine  
711 phytoplankton during photosynthesis. *Plant Cell Environ.* 13, 207–218.  
712 <https://doi.org/10.1111/j.1365-3040.1990.tb01305.x>

713 Dittmar, T., 2015. Reasons Behind the Long-Term Stability of Dissolved Organic Matter, in:  
714 Biogeochemistry of Marine Dissolved Organic Matter. Elsevier, pp. 369–388.  
715 <https://doi.org/10.1016/B978-0-12-405940-5.00007-8>

716 Ducklow, H.W., Hansell, D.A., Morgan, J.A., 2007. Dissolved organic carbon and nitrogen in the  
717 Western Black Sea. *Mar. Chem.* 105, 140–150. <https://doi.org/10.1016/j.marchem.2007.01.015>

718 Erez, J., Bouevitch, A., Kaplan, A., 1998. Carbon isotope fractionation by photosynthetic aquatic  
719 microorganisms: experiments with *Synechococcus* PCC7942, and a simple carbon flux model. *Can. J.*  
720 *Bot.* 76, 1109–1118. <https://doi.org/10.1139/b98-067>

721 Fakhraee, M., Tarhan, L.G., Planavsky, N.J., Reinhard, C.T., 2021. A largely invariant marine dissolved  
722 organic carbon reservoir across Earth’s history. *Proc. Natl. Acad. Sci.* 118, e2103511118.  
723 <https://doi.org/10.1073/pnas.2103511118>

724 Ferrari, L., Orozco-Esquivel, T., Manea, V., Manea, M., 2012. The dynamic history of the Trans-  
725 Mexican Volcanic Belt and the Mexico subduction zone. *Tectonophysics* 522–523, 122–149.  
726 <https://doi.org/10.1016/j.tecto.2011.09.018>

727 Fike, D.A., Grotzinger, J.P., Pratt, L.M., Summons, R.E., 2006. Oxidation of the Ediacaran Ocean.  
728 *Nature* 444, 744–747. <https://doi.org/10.1038/nature05345>

729 Fogel, M.L., Cifuentes, L.A., 1993. Isotope Fractionation during Primary Production, in: Engel, M.H.,  
730 Macko, S.A. (Eds.), *Organic Geochemistry, Topics in Geobiology*. Springer US, Boston, MA, pp. 73–98.  
731 [https://doi.org/10.1007/978-1-4615-2890-6\\_3](https://doi.org/10.1007/978-1-4615-2890-6_3)

732 Fry, B., 1996.  $^{13}\text{C}/^{12}\text{C}$  fractionation by marine diatoms. *Mar. Ecol. Prog. Ser.* 134, 283–294.  
733 <https://doi.org/10.3354/meps134283>

734 Hansell, D.A., 2013. Recalcitrant Dissolved Organic Carbon Fractions. *Annu. Rev. Mar. Sci.* 5, 421–445.  
735 <https://doi.org/10.1146/annurev-marine-120710-100757>

736 Havig, J.R., Hamilton, T.L., McCormick, M., McClure, B., Sowers, T., Wegter, B., Kump, L.R., 2018.  
737 Water column and sediment stable carbon isotope biogeochemistry of permanently redox-stratified  
738 Fayetteville Green Lake, New York, U.S.A. *Limnol. Oceanogr.* 63, 570–587.  
739 <https://doi.org/10.1002/lno.10649>

740 Havig, J.R., McCormick, M.L., Hamilton, T.L., Kump, L.R., 2015. The behavior of biologically important  
741 trace elements across the oxic/euxinic transition of meromictic Fayetteville Green Lake, New York,  
742 USA. *Geochim. Cosmochim. Acta* 165, 389–406. <https://doi.org/10.1016/j.gca.2015.06.024>

743 Hayes, J.M., 2001. Fractionation of Carbon and Hydrogen Isotopes in Biosynthetic Processes\*. *Rev.*  
744 *Mineral. Geochem.* 43, 225–277. <https://doi.org/10.2138/gsrmg.43.1.225>

745 Hessen, D.O., 1992. Dissolved organic carbon in a humic lake: effects on bacterial production and  
746 respiration, in: Salonen, K., Kairesalo, T., Jones, R.I. (Eds.), *Dissolved Organic Matter in Lacustrine*  
747 *Ecosystems: Energy Source and System Regulator, Developments in Hydrobiology*. Springer  
748 Netherlands, Dordrecht, pp. 115–123. [https://doi.org/10.1007/978-94-011-2474-4\\_9](https://doi.org/10.1007/978-94-011-2474-4_9)

749 Hessen, D.O., Anderson, T.R., 2008. Excess carbon in aquatic organisms and ecosystems:  
750 Physiological, ecological, and evolutionary implications. *Limnol. Oceanogr.* 53, 1685–1696.  
751 <https://doi.org/10.4319/lo.2008.53.4.1685>

752 Iniesto, M., Moreira, D., Benzerara, K., Reboul, G., Bertolino, P., Tavera, R., López-García, P., 2022.  
753 Planktonic microbial communities from microbialite-bearing lakes sampled along a salinity-alkalinity  
754 gradient. *Limnol. Oceanogr.* Ino.12233. <https://doi.org/10.1002/Ino.12233>

755 Iñiguez, C., Capó-Bauçà, S., Niinemets, Ü., Stoll, H., Aguiló-Nicolau, P., Galmés, J., 2020. Evolutionary  
756 trends in RuBisCO kinetics and their co-evolution with CO<sub>2</sub> concentrating mechanisms. *Plant J.* 101,  
757 897–918. <https://doi.org/10.1111/tpj.14643>

758 Ivanovsky, R.N., Lebedeva, N.V., Keppen, O.I., Chudnovskaya, A.V., 2020. Release of  
759 Photosynthetically Fixed Carbon as Dissolved Organic Matter by Anoxygenic Phototrophic Bacteria.  
760 *Microbiology* 89, 28–34. <https://doi.org/10.1134/S0026261720010075>

761 Jiang, G., Wang, X., Shi, X., Xiao, S., Zhang, S., Dong, J., 2012. The origin of decoupled carbonate and  
762 organic carbon isotope signatures in the early Cambrian (ca. 542–520Ma) Yangtze platform. *Earth  
763 Planet. Sci. Lett.* 317–318, 96–110. <https://doi.org/10.1016/j.epsl.2011.11.018>

764 Jiang, G., Wang, X., Shi, X., Zhang, S., Xiao, S., Dong, J., 2010. Organic carbon isotope constraints on  
765 the dissolved organic carbon (DOC) reservoir at the Cryogenian–Ediacaran transition. *Earth Planet.  
766 Sci. Lett.* 299, 159–168. <https://doi.org/10.1016/j.epsl.2010.08.031>

767 Jiao, N., Herndl, G.J., Hansell, D.A., Benner, R., Kattner, G., Wilhelm, S.W., Kirchman, D.L., Weinbauer,  
768 M.G., Luo, T., Chen, F., Azam, F., 2010. Microbial production of recalcitrant dissolved organic matter:  
769 long-term carbon storage in the global ocean. *Nat. Rev. Microbiol.* 8, 593–599.  
770 <https://doi.org/10.1038/nrmicro2386>

771 Kaplan, L.A., Wiegner, T.N., Newbold, J.D., Ostrom, P.H., Gandhi, H., 2008. Untangling the complex  
772 issue of dissolved organic carbon uptake: a stable isotope approach. *Freshw. Biol.* 53, 855–864.  
773 <https://doi.org/10.1111/j.1365-2427.2007.01941.x>

774 Kawasaki, N., Komatsu, K., Kohzu, A., Tomioka, N., Shinohara, R., Satou, T., Watanabe, F.N., Tada, Y.,  
775 Hamasaki, K., Kushairi, M.R.M., Imai, A., 2013. Bacterial Contribution to Dissolved Organic Matter in  
776 Eutrophic Lake Kasumigaura, Japan. *Appl. Environ. Microbiol.* 79, 7160–7168.  
777 <https://doi.org/10.1128/AEM.01504-13>

778 Kroopnick, P.M., 1985. The distribution of <sup>13</sup>C of ΣCO<sub>2</sub> in the world oceans. *Deep Sea Research Part  
779 A. Oceanographic Research Papers*, 32(1), pp.57-84. [https://doi.org/10.1016/0198-0149\(85\)90017-2](https://doi.org/10.1016/0198-0149(85)90017-2)

780 Kuntz, L.B., Laakso, T.A., Schrag, D.P., Crowe, S.A., 2015. Modeling the carbon cycle in Lake Matano.  
781 *Geobiology* 13, 454–461. <https://doi.org/10.1111/gbi.12141>

782 Lampert, W., 1978. Release of dissolved organic carbon by grazing zooplankton. *Limnol. Oceanogr.*  
783 23, 831–834. <https://doi.org/10.4319/lo.1978.23.4.0831>

784 Lehmann, M.F., Bernasconi, S.M., Barbieri, A., McKenzie, J.A., 2002. Preservation of organic matter  
785 and alteration of its carbon and nitrogen isotope composition during simulated and in situ early  
786 sedimentary diagenesis. *Geochim. Cosmochim. Acta* 66, 3573–3584. [https://doi.org/10.1016/S0016-7037\(02\)00968-7](https://doi.org/10.1016/S0016-7037(02)00968-7)

788 Lenton, T.M., Daines, S.J., 2018. The effects of marine eukaryote evolution on phosphorus, carbon  
789 and oxygen cycling across the Proterozoic–Phanerozoic transition. *Emerg. Top. Life Sci.* 2, 267–278.  
790 <https://doi.org/10.1042/ETLS20170156>

791 Lenton, T.M., Daines, S.J., 2017. Matworld – the biogeochemical effects of early life on land. *New  
792 Phytol.* 215, 531–537. <https://doi.org/10.1111/nph.14338>

793 Li, C., Hardisty, D.S., Luo, G., Huang, J., Algeo, T.J., Cheng, M., Shi, W., An, Z., Tong, J., Xie, S., Jiao, N.,  
794 Lyons, T.W., 2017. Uncovering the spatial heterogeneity of Ediacaran carbon cycling. *Geobiology* 15,  
795 211–224. <https://doi.org/10.1111/gbi.12222>

796 Lu, M., Zhu, M., Zhang, J., Shields-Zhou, G., Li, G., Zhao, F., Zhao, X., Zhao, M., 2013. The DOUNCE  
797 event at the top of the Ediacaran Doushantuo Formation, South China: Broad stratigraphic  
798 occurrence and non-diagenetic origin. *Precambrian Res.* 225, 86–109.  
799 <https://doi.org/10.1016/j.precamres.2011.10.018>

800 Lugo, A., Alcocer, J., Sanchez, M.R., Escobar, E., 1993. Trophic status of tropical lakes indicated by  
801 littoral protozoan assemblages. *SIL Proc.* 1922-2010 25, 441–443.  
802 <https://doi.org/10.1080/03680770.1992.11900159>

803 Lyons, T.W., Reinhard, C.T., Planavsky, N.J., 2014. The rise of oxygen in Earth’s early ocean and  
804 atmosphere. *Nature* 506, 307–315. <https://doi.org/10.1038/nature13068>

805 Macek, M., Medina, X.S., Picazo, A., Peřtová, D., Reyes, F.B., Hernández, J.R.M., Alcocer, J., Ibarra,  
806 M.M., Camacho, A., 2020. Spirostomum teres: A Long Term Study of an Anoxic-Hypolimnion  
807 Population Feeding upon Photosynthesizing Microorganisms. *Acta Protozool.* 59, 13–38.  
808 <https://doi.org/10.4467/16890027AP.20.002.12158>

809 Marañoń, E., Cermeño, P., Fernández, E., Rodríguez, J., Zabala, L., 2004. Significance and mechanisms  
810 of photosynthetic production of dissolved organic carbon in a coastal eutrophic ecosystem. *Limnol.  
811 Oceanogr.* 49, 1652–1666. <https://doi.org/10.4319/lo.2004.49.5.1652>

812 Margolin, A.R., Gerringa, L.J.A., Hansell, D.A., Rijkenberg, M.J.A., 2016. Net removal of dissolved  
813 organic carbon in the anoxic waters of the Black Sea. *Mar. Chem.* 183, 13–24.  
814 <https://doi.org/10.1016/j.marchem.2016.05.003>

815 Morana, C., Sarmiento, H., Descy, J.-P., Gasol, J.M., Borges, A.V., Bouillon, S., Darchambeau, F., 2014.  
816 Production of dissolved organic matter by phytoplankton and its uptake by heterotrophic  
817 prokaryotes in large tropical lakes. *Limnol. Oceanogr.* 59, 1364–1375.  
818 <https://doi.org/10.4319/lo.2014.59.4.1364>

819 Organization for Economic Cooperation and Development (OECD), 1982, Eutrophication of waters.  
820 Monitoring, assessment and control: Paris, Organization for Economic Cooperation and  
821 Development, 154 p.

822 Ogawa, H., Amagai, Y., Koike, I., Kaiser, K., Benner, R., 2001. Production of Refractory Dissolved  
823 Organic Matter by Bacteria. *Science* 292, 917–920. <https://doi.org/10.1126/science.1057627>

824 O’Leary, M.H., 1988. Carbon Isotopes in Photosynthesis. *BioScience* 38, 328–336.  
825 <https://doi.org/10.2307/1310735>

826 Otero, A., Vincenzini, M., 2003. Extracellular polysaccharide synthesis by Nostoc strains as affected  
827 by N source and light intensity. *J. Biotechnol.* 102, 143–152. [https://doi.org/10.1016/S0168-  
828 1656\(03\)00022-1](https://doi.org/10.1016/S0168-1656(03)00022-1)

829 Peltier, W.R., Liu, Y., Crowley, J.W., 2007. Snowball Earth prevention by dissolved organic carbon  
830 remineralization. *Nature* 450, 813–818. <https://doi.org/10.1038/nature06354>

831 Petrash, D.A., Steenbergen, I.M., Valero, A., Meador, T.B., Pačes, T., Thomazo, C., 2022. Aqueous  
832 system-level processes and prokaryote assemblages in the ferruginous and sulfate-rich bottom  
833 waters of a post-mining lake. *Biogeosciences* 19, 1723–1751. [https://doi.org/10.5194/bg-19-1723-](https://doi.org/10.5194/bg-19-1723-2022)  
834 2022

835 Posth, N.R., Bristow, L.A., Cox, R.P., Habicht, K.S., Danza, F., Tonolla, M., Frigaard, N. -U., Canfield,  
836 D.E., 2017. Carbon isotope fractionation by anoxygenic phototrophic bacteria in euxinic Lake  
837 Cadagno. *Geobiology* 15, 798–816. <https://doi.org/10.1111/gbi.12254>

838 Rao, D.N., Chopra, M., Rajula, G.R., Durgadevi, D.S.L., Sarma, V.V.S.S., 2021. Release of significant  
839 fraction of primary production as dissolved organic carbon in the Bay of Bengal. *Deep Sea Res. Part*  
840 *Oceanogr. Res. Pap.* 168, 103445. <https://doi.org/10.1016/j.dsr.2020.103445>

841 Renstrom-Kellner, E., Bergman, B., 1989. Glycolate metabolism in cyanobacteria. III. Nitrogen  
842 controls excretion and metabolism of glycolate in *Anabaena cylindrica*. *Physiol. Plant.* 77, 46–51.  
843 <https://doi.org/10.1111/j.1399-3054.1989.tb05976.x>

844 Repeta, D.J., Aluwihare, L.I., 2006. Radiocarbon analysis of neutral sugars in high-molecular-weight  
845 dissolved organic carbon: Implications for organic carbon cycling. *Limnol. Oceanogr.* 51, 1045–1053.  
846 <https://doi.org/10.4319/lo.2006.51.2.1045>

847 Ridgwell, A., Arndt, S., 2015. Chapter 1 - Why Dissolved Organics Matter: DOC in Ancient Oceans and  
848 Past Climate Change, in: Hansell, D.A., Carlson, C.A. (Eds.), *Biogeochemistry of Marine Dissolved*  
849 *Organic Matter (Second Edition)*. Academic Press, Boston, pp. 1–20. [https://doi.org/10.1016/B978-0-](https://doi.org/10.1016/B978-0-12-405940-5.00001-7)  
850 12-405940-5.00001-7

851 Riebesell, U., Burkhardt, S., Dauelsberg, A., Kroon, B., 2000. Carbon isotope fractionation by a marine  
852 diatom: dependence on the growth-rate-limiting resource. *Mar. Ecol. Prog. Ser.* 193, 295–303.  
853 <https://doi.org/10.3354/meps193295>

854 Rothman, D.H., Hayes, J.M., Summons, R.E., 2003. Dynamics of the Neoproterozoic carbon cycle.  
855 *Proc. Natl. Acad. Sci.* 100, 8124–8129. <https://doi.org/10.1073/pnas.0832439100>

856 Saini, J.S., Hassler, C., Cable, R., Fourquez, M., Danza, F., Roman, S., Tonolla, M., Storelli, N., Jacquet,  
857 S., Zdobnov, E.M., Duhaime, M.B., 2021. Microbial loop of a Proterozoic ocean analogue (preprint).  
858 *Microbiology*. <https://doi.org/10.1101/2021.08.17.456685>

859 Saltzman, M.R., Thomas, E., 2012. Carbon Isotope Stratigraphy, in: *The Geologic Time Scale*. Elsevier,  
860 pp. 207–232. <https://doi.org/10.1016/B978-0-444-59425-9.00011-1>

861 Santinelli, C., Follett, C., Retelletti Brogi, S., Xu, L., Repeta, D., 2015. Carbon isotope measurements  
862 reveal unexpected cycling of dissolved organic matter in the deep Mediterranean Sea. *Mar. Chem.*  
863 177, 267–277. <https://doi.org/10.1016/j.marchem.2015.06.018>

864 Satkoski, A.M., Beukes, N.J., Li, W., Beard, B.L., Johnson, C.M., 2015. A redox-stratified ocean 3.2  
865 billion years ago. *Earth Planet. Sci. Lett.* 430, 43–53. <https://doi.org/10.1016/j.epsl.2015.08.007>

866 Schiff, S.L., Tsuji, J.M., Wu, L., Venkiteswaran, J.J., Molot, L.A., Elgood, R.J., Paterson, M.J., Neufeld,  
867 J.D., 2017. Millions of Boreal Shield Lakes can be used to Probe Archaean Ocean Biogeochemistry.  
868 *Sci. Rep.* 7, 46708. <https://doi.org/10.1038/srep46708>

869 Sexton, P.F., Norris, R.D., Wilson, P.A., Pälike, H., Westerhold, T., Röhl, U., Bolton, C.T., Gibbs, S.,  
870 2011. Eocene global warming events driven by ventilation of oceanic dissolved organic carbon.  
871 Nature 471, 349–352. <https://doi.org/10.1038/nature09826>

872 Shi, W., Li, C., Algeo, T.J., 2017. Quantitative model evaluation of organic carbon oxidation  
873 hypotheses for the Ediacaran Shuram carbon isotopic excursion. Sci. China Earth Sci. 60, 2118–2127.  
874 <https://doi.org/10.1007/s11430-017-9137-1>

875 Shields, G.A., Mills, B.J.W., Zhu, M., Raub, T.D., Daines, S.J., Lenton, T.M., 2019. Unique  
876 Neoproterozoic carbon isotope excursions sustained by coupled evaporite dissolution and pyrite  
877 burial. Nat. Geosci. 12, 823–827. <https://doi.org/10.1038/s41561-019-0434-3>

878 Siebe, C., Guilbaud, M.-N., Salinas, S., Chédeville-Monzo, C., 2012. Eruption of Alberca de los Espinos  
879 tuff cone causes transgression of Zacapu lake ca. 25,000 yr BP in Michoacán, México. Presented at  
880 the IAS 4IMC Conference, Auckland, New Zeland, pp. 74–75.

881 Siebe, C., Guilbaud, M.-N., Salinas, S., Kshirsagar, P., Chevrel, M.O., Jiménez, A.H., Godínez, L., 2014.  
882 Monogenetic volcanism of the Michoacán-Guanajuato Volcanic Field: Maar craters of the Zacapu  
883 basin and domes, shields, and scoria cones of the Tarascan highlands (Paracho-Paricutin region).  
884 Presented at the Pre-meeting field guide for the 5th international Maar Conference, Querétaro,  
885 México, pp. 1–37.

886 Sigala, I., Caballero, M., Correa-Metrio, A., Lozano-García, S., Vázquez, G., Pérez, L., Zawisza, E., 2017.  
887 Basic limnology of 30 continental waterbodies of the Transmexican Volcanic Belt across climatic and  
888 environmental gradients. Bol. Soc. Geológica Mex. 69, 313–370.  
889 <https://doi.org/10.18268/BSGM2017v69n2a3>

890 Silva-Aguilera, R.A., Vilaclara, G., Armienta, M.A., Escolero, Ó., 2022. Hydrogeology and  
891 Hydrochemistry of the Serdán-Oriental Basin and the Lake Alchichica, in: Alcocer, J. (Ed.), Lake  
892 Alchichica Limnology. Springer International Publishing, Cham, pp. 63–74.  
893 [https://doi.org/10.1007/978-3-030-79096-7\\_5](https://doi.org/10.1007/978-3-030-79096-7_5)

894 Sperling, E.A., Peterson, K.J., Laflamme, M., 2011. Rangeomorphs, Thectardis (Porifera?) and  
895 dissolved organic carbon in the Ediacaran oceans: Rangeomorphs, Thectardis and DOC. Geobiology 9,  
896 24–33. <https://doi.org/10.1111/j.1472-4669.2010.00259.x>

897 Swanson-Hysell, N.L., Rose, C.V., Calmet, C.C., Halverson, G.P., Hurtgen, M.T., Maloof, A.C., 2010.  
898 Cryogenian Glaciation and the Onset of Carbon-Isotope Decoupling. Science 328, 608–611.  
899 <https://doi.org/10.1126/science.1184508>

900 Thomas, P.J., Boller, A.J., Satagopan, S., Tabita, F.R., Cavanaugh, C.M., Scott, K.M., 2019. Isotope  
901 discrimination by form IC RubisCO from *Ralstonia eutropha* and *Rhodobacter sphaeroides* ,  
902 metabolically versatile members of ‘ *Proteobacteria* ’ from aquatic and soil habitats. Environ.  
903 Microbiol. 21, 72–80. <https://doi.org/10.1111/1462-2920.14423>

904 Thornton, D.C.O., 2014. Dissolved organic matter (DOM) release by phytoplankton in the  
905 contemporary and future ocean. Eur. J. Phycol. 49, 20–46.  
906 <https://doi.org/10.1080/09670262.2013.875596>

907 Tziperman, E., Halevy, I., Johnston, D.T., Knoll, A.H., Schrag, D.P., 2011. Biologically induced initiation  
908 of Neoproterozoic snowball-Earth events. Proc. Natl. Acad. Sci. 108, 15091–15096.  
909 <https://doi.org/10.1073/pnas.1016361108>

910 Vilaclara, G., Chávez, M., Lugo, A., González, H., Gaytán, M., 1993. Comparative description of crater-  
911 lakes basic chemistry in Puebla State, Mexico. *SIL Proc.* 1922-2010 25, 435–440.  
912 <https://doi.org/10.1080/03680770.1992.11900158>

913 Wagner, S., Schubotz, F., Kaiser, K., Hallmann, C., Waska, H., Rossel, P.E., Hansman, R., Elvert, M.,  
914 Middelburg, J.J., Engel, A., Blattmann, T.M., Catalá, T.S., Lennartz, S.T., Gomez-Saez, G.V., Pantoja-  
915 Gutiérrez, S., Bao, R., Galy, V., 2020. Soothsaying DOM: A Current Perspective on the Future of  
916 Oceanic Dissolved Organic Carbon. *Front. Mar. Sci.* 7, 341. <https://doi.org/10.3389/fmars.2020.00341>

917 Werne, J.P., Hollander, D.J., 2004. Balancing supply and demand: controls on carbon isotope  
918 fractionation in the Cariaco Basin (Venezuela) Younger Dryas to present. *Mar. Chem.* 92, 275–293.  
919 <https://doi.org/10.1016/j.marchem.2004.06.031>

920 Wetz, M.S., Wheeler, P.A., 2007. Release of dissolved organic matter by coastal diatoms. *Limnol.*  
921 *Oceanogr.* 52, 798–807. <https://doi.org/10.4319/lo.2007.52.2.0798>

922 Williams, P.M., Gordon, L.I., 1970. Carbon-13: carbon-12 ratios in dissolved and particulate organic  
923 matter in the sea. *Deep Sea Res. Oceanogr. Abstr.* 17, 19–27. [https://doi.org/10.1016/0011-](https://doi.org/10.1016/0011-7471(70)90085-9)  
924 [7471\(70\)90085-9](https://doi.org/10.1016/0011-7471(70)90085-9)

925 Xing, C., Liu, P., Wang, R., Li, C., Li, J., Shen, B., 2022. Tracing the evolution of dissolved organic  
926 carbon (DOC) pool in the Ediacaran ocean by Germanium/silica (Ge/Si) ratios of diagenetic chert  
927 nodules from the Doushantuo Formation, South China. *Precambrian Res.* 374, 106639.  
928 <https://doi.org/10.1016/j.precamres.2022.106639>

929 Zeebe, R.E., Wolf-Gladrow, D.A. (2009). Carbon Dioxide, Dissolved (Ocean). In: Gornitz, V. (eds)  
930 *Encyclopedia of Paleoclimatology and Ancient Environments.* Encyclopedia of Earth Sciences Series.  
931 Springer, Dordrecht. [https://doi.org/10.1007/978-1-4020-4411-3\\_30](https://doi.org/10.1007/978-1-4020-4411-3_30)

932 Zeyen, N., Benzerara, K., Beyssac, O., Daval, D., Muller, E., Thomazo, C., Tavera, R., López-García, P.,  
933 Moreira, D., Duprat, E., 2021. Integrative analysis of the mineralogical and chemical composition of  
934 modern microbialites from ten Mexican lakes: What do we learn about their formation? *Geochim.*  
935 *Cosmochim. Acta* 305, 148–184. <https://doi.org/10.1016/j.gca.2021.04.030>

936